Received: 10 February 2023 | Revised: 4 April 2023 | Accepted: 10 April 2023

DOI: 10.1002/jmor.21591

RESEARCH ARTICLE

JOURNAL OF morphology WILEY

The relative contributions of multiarticular snake muscles to movement in different planes

Jessica L. Tingle[1] | Derek J. Jurestovsky[1,2] | Henry C. Astley[1]

[1]Department of Biology, University of Akron, Akron, Ohio, USA

[2]Department of Kinesiology, Biomechanics Laboratory, Pennsylvania State University, Pennsylvania, USA

Correspondence

Jessica L. Tingle, Department of Biology, University of Akron, Akron, OH 44325, USA, Email: jessica.tingle@email.ucr.edu

Present addresses

Derek J. Jurestovsky, Department of Kinesiology, Biomechanics Laboratory, Pennsylvania State University, Pennsylvania, USA; and Department of Kinesiology, Biomechanics Laboratory, Pennsylvania State University, Pennsylvania, USA.

Funding information

National Science Foundation

Abstract

Muscles spanning multiple joints play important functional roles in a wide range of systems across tetrapods; however, their fundamental mechanics are poorly understood, particularly the consequences of anatomical position on mechanical advantage. Snakes provide an excellent study system for advancing this topic. They rely on the axial muscles for many activities, including striking, constriction, defensive displays, and locomotion. Moreover, those muscles span from one or a few vertebrae to over 30, and anatomy varies among muscles and among species. We characterized the anatomy of major epaxial muscles in a size series of corn snakes (*Pantherophis guttatus*) using diceCT scans, and then took several approaches to calculating contributions of each muscle to force and motion generated during body bending, starting from a highly simplistic model and moving to increasingly complex and realistic models. Only the most realistic model yielded equations that included the consequence of muscle span on torque-displacement trade-offs, as well as resolving ambiguities that arose from simpler models. We also tested whether muscle cross-sectional areas or lever arms (total magnitude or pitch/yaw/roll components) were related to snake mass, longitudinal body region (anterior, middle, posterior), and/or muscle group (semispinalis-spinalis, multifidus, longissimus dorsi, iliocostalis, and levator costae). Muscle cross-sectional areas generally scaled with positive allometry, and most lever arms did not depart significantly from geometric similarity (isometry). The levator costae had lower cross-sectional area than the four epaxial muscles, which did not differ significantly from each other in cross-sectional area. Lever arm total magnitudes and components differed among muscles. We found some evidence for regional variation, indicating that functional regionalization merits further investigation. Our results contribute to knowledge of snake muscles specifically and multiarticular muscle systems generally, providing a foundation for future comparisons across species and bioinspired multiarticular systems.

KEYWORDS
allometry, biomechanics, functional morphology, range of motion, squamates, vertebrates

1 | INTRODUCTION

Muscles spanning two or more joints play important functional roles in a huge diversity of systems across tetrapod vertebrates. Some familiar examples include bi-articular muscles in the limbs, such as the hamstring and gastrocnemius, which play an important role in joint coordination and power transfer (Aerts, 1998; Bobbert & van Ingen Schenau, 1988; Bodine et al., 1982; van Ingen Schenau et al., 1994; van Ingen Schenau, 1989). Tetrapod species from humans to frogs owe their manual dexterity to muscles spanning multiple finger or hand joints (Manzano et al., 2008; Sustaita et al., 2013; Valero-Cuevas, 2005), and some species, particularly birds, have evolved similarly dexterous systems in their feet (Backus et al., 2015; Sustaita et al., 2013). Parts of the vertebral column, with numerous muscles crossing multiple vertebrae, have also been co-opted for grasping or manipulating objects: such disparate clades as monkeys and chameleons have independently evolved prehensile tails (Lemelin, 1995; Luger et al., 2020, 2021; Organ, 2007), while some birds have highly mobile necks to compensate for having turned their forelimbs into wings (Böhmer et al., 2020; van der Leeuw et al., 2001).

Beyond object manipulation and prehension, some multiarticular muscle systems function in force production and/or postural control during locomotor tasks. Many tetrapod trunk muscles span multiple vertebrae, contributing both to bending and to stabilization of the vertebral column during swimming and quadrupedal locomotion (Gramsbergen et al., 1999; Omura et al., 2015; O'Reilly et al., 2000; Ritter, 1992; Schilling & Carrier, 2010). Humans have similarly multiarticular trunk muscles (Dumas et al., 1991; Macintosh et al., 1993) that we rely on for their crucial roles, including force production for movement and postural stability during walking, running, lifting, squatting, and other exercises (Cholewicki & VanVliet IV, 2002; Cromwell et al., 2001; Kong et al., 2013; Nuzzo et al., 2008; Saunders et al., 2004). Numerous tetrapod lineages have foregone limbs entirely, evolving elongate body plans that rely on multiarticular trunk muscles for axial propulsion on land (Bergmann et al., 2020; Wiens et al., 2006).

Not only do multiarticular muscles merit the attention of organismal biologists due to their ubiquitous and diverse roles, but their study could also have clinical and engineering applications. For example, some medical treatments and prostheses rely upon understanding complex multiarticular systems such as the hand (Adamczyk & Crago, 2000; Lee et al., 2018; Valero-Cuevas, 2005). Additionally, bioinspired design based on multiarticular muscle systems can enhance the capabilities of slithering snake-like robots, robotic tails to stabilize wheeled or limbed robots, perching rotorcraft, and grasping robot manipulators, among other devices (Doyle et al., 2013; Kano et al., 2011; Pollard & Gilbert, 2002; Ramos & Walker, 1998; Saab et al., 2018).

Despite the importance of multiarticular muscle systems for both organismal biology and applied science, we still have only a limited understanding of many topics related to their function. Of these, a fundamental topic in need of study is the relationship between musculoskeletal anatomy and functional outputs, particularly the mechanical advantage of such systems.

Snakes provide an excellent opportunity for studying numerous aspects of multiarticular systems. Anatomical descriptions of axial muscles in numerous species demonstrate that some of their muscles have modest spans of several vertebrae while others span far more, sometimes upwards of 30–40 vertebrae; moreover, muscle architecture varies among muscles and among species; see Figure 1a for a diagram of several muscles of interest). Many multiarticular systems are dedicated to a primary task, such as grasping or manipulating objects (human fingers, bird feet, chameleon tails) or postural stability (human trunk muscles). In contrast, snakes rely on their axial musculoskeletal system for a huge diversity of activities, including striking, constriction, grasping, defensive displays, and locomotion. Not limited to one or even a few types of locomotion, snakes can move in far more ways than most appreciate (Jayne, 2020), and even their most common gait, lateral undulation, displays vast kinematic variability (Astley & Jayne, 2009; Gray & Lissmann, 1950; Jayne, 2020; Schiebel et al., 2020). This behavioral variability, along with correlations of muscle length with habitat and locomotion (Jayne, 1982; Tingle et al., 2017), suggest functional consequences of anatomical differences. However, few studies have examined the function of snake muscles during locomotion or other activities (Jayne, 1988a, 1988b; Newman & Jayne, 2018), and fewer have attempted to provide theory or models demonstrating how snake muscle anatomy contributes to function (Astley, 2020; Ruben, 1977). Additional work linking muscle anatomy to function in snakes would not only increase our knowledge of this highly successful clade of animals, but it would also improve our general understanding of how a multiarticular muscle system can be arranged to meet multiple demands.

The present study focuses on basic biomechanics in the corn snake, *Pantherophis guttatus*. We had three major aims with respect to the major epaxial muscles and one hypaxial muscle: 1) determine the relative contributions of muscles to bending torque by calculating their cross-sectional areas and lever arms;

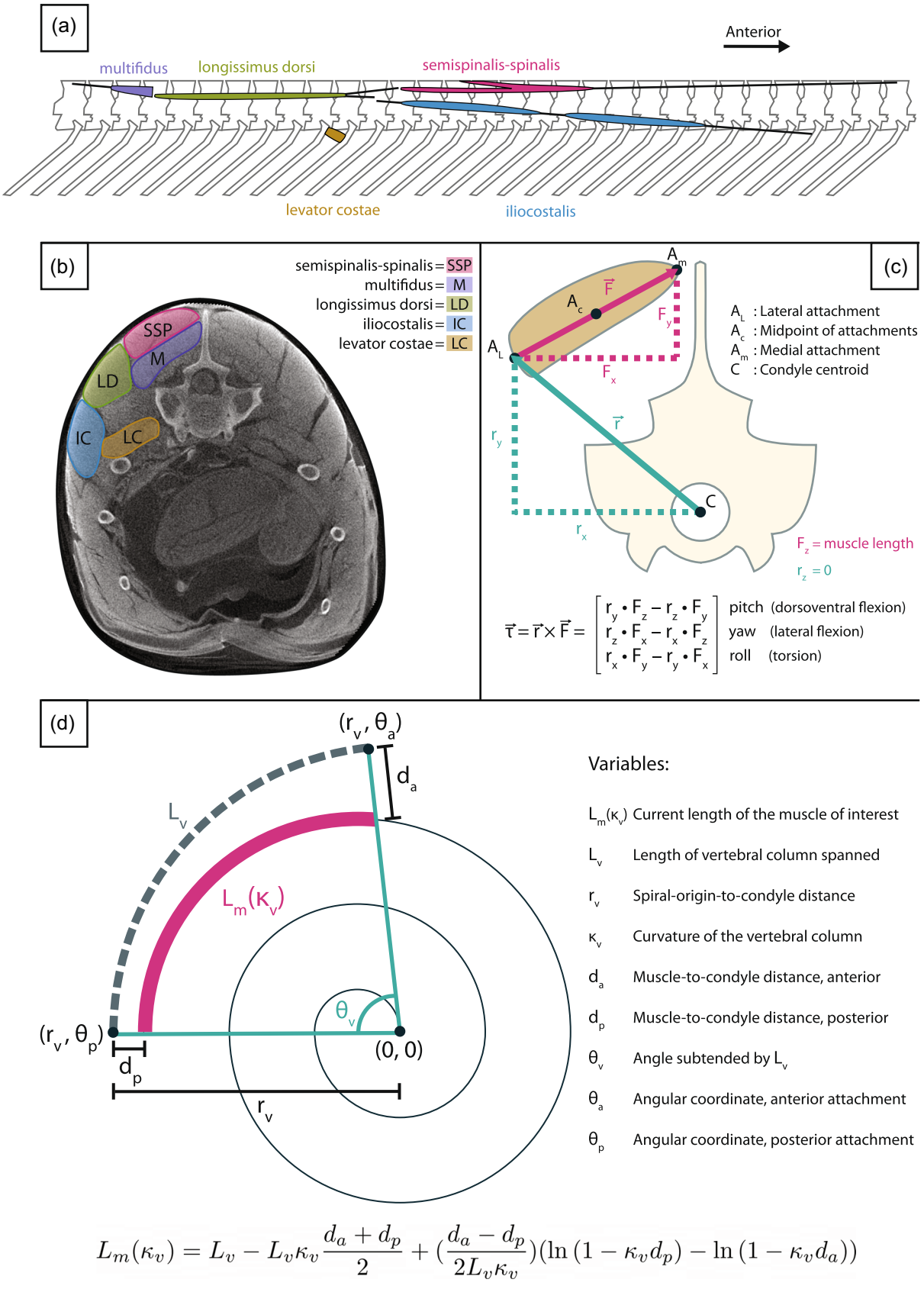

$$L_m(\kappa_v) = L_v - L_v\kappa_v\frac{d_a + d_p}{2} + \left(\frac{d_a - d_p}{2L_v\kappa_v}\right)\left(\ln\left(1 - \kappa_v d_p\right) - \ln\left(1 - \kappa_v d_a\right)\right)$$

FIGURE 1 (See caption on next page)

2) determine whether muscle cross-sectional areas and/or lever arms vary along the body axis; 3) examine scaling of muscle cross-sectional area and lever arms.

2 | MATERIALS AND METHODS

2.1 | Specimen preparation and micro-CT scanning

Our sample consisted of six wild-caught corn snakes, *Pantherophis guttatus* (Linnaeus, 1766) representing a size range of juveniles and adults weighing 50 g, 80 g, 135 g, 180 g, 265 g, and 335 g, measured immediately before euthanasia. Their snout-vent lengths and total lengths (SVL/TL) were 550/670 mm, 695/800 mm, 805/920 mm, 755/900 mm, 870/1040 mm, and 1010/1180 mm, respectively, measured immediately after euthanasia. Their mid-body widths were 11 mm, 12 mm, 17 mm, 17 mm, 19 mm, and 19 mm, respectively, measured from preserved specimens. These six individuals were also used in a previous study (Jurestovsky et al., 2022). The snakes were purchased from a commercial provider and kept under University of Akron IACUC protocol # 16-08-16-ASD. We euthanized them with MS222 following the protocol of Conroy et al. (2009). Before rigor mortis set in, we pinned them into a position that produced several straight sections (for ease of μCT scanning) and preserved them with formalin (Jurestovsky et al., 2022). Pins were placed along the outside of the body so as not to damage muscle tissue. We later rinsed the specimens in deionized water and placed them in ethanol for preservation. After preservation, we cut the snakes into several sections. Some of the sections were used in a separate study to examine muscle sarcomere lengths (Jurestovsky et al., 2022). For this study, we used three straight sections per snake taken slightly posterior to 25%, 50%, and 75% snout-vent length (SVL). Previous studies have not found evidence for substantial among-individual variation within species, or substantial regional variation, except at the extreme anterior and posterior ends of the body where muscle-tendon units necessarily span fewer joints (Jayne, 1982; Nicodemo, 2012; Pregill, 1977). The sections were skinned and stained with a solution of 5% phosphomolybdic acid (PMA) in deionized water for approximately 3 weeks (Gignac et al., 2016). We chose a PMA solution for staining because initial attempts to stain a specimen with iodine led to an unacceptable level of muscle tissue shrinkage and substantial specimen distortion (Gignac et al., 2016). After staining, the sections were μCT scanned (SkyScan 1172, 80–100 kV, 100–120 μA, 10.99–26.16 μm voxels, depending on specimen size; Bruker). All scans were uploaded to MorphoSource as image stacks (see Supporting Information File 1 for DOIs).

2.2 | Anatomical data

We used the Fiji distribution of ImageJ 1.53t, Java 1.8.0_172 (Schindelin et al., 2012) to quantify vertebral and muscle anatomy from transverse sections (slices) of μCT scans (Figure 1b). To determine vertebral length, we chose a feature that could be precisely located in consecutive vertebrae, the posterior edge of the postzygapophysis, and counted the number of μCT scan slices between them. We then multiplied the number of slices by the voxel size to get vertebral length in mm. In this way, we measured the length of 6-9 vertebrae for each scanned snake section. To determine the number of vertebrae spanned by several muscles of interest, we dissected a midbody section of a formalin-fixed and ethanol-preserved 510 g corn snake.

Fiji's oval selection function allowed us to outline the condyle, and the polygon selection function allowed us to outline several muscles of interest: the semispinalis-spinalis along with its anterior tendon bundle, the multifidus, the longissimus dorsi, the iliocostalis, and the levator costae (Figure 1b). We used Fiji's measurement function to compute the cross-sectional area and centroid x and y coordinates for each of these regions. Additionally, we used the point function to get the x and y coordinates of several landmarks of interest: the top of the neural spine, the most lateral points visible on the left and right prezygapophyses, and our best estimates of medial and/or lateral attachment points of muscles for which we determined the muscle centroid was not the best estimate of one or both attachment points based on published anatomical drawings (Gasc,1974, 1981; Table 1). The anatomy output from Fiji can be found in Supporting Information material File 2, and additional raw data used for analysis can be found in Supporting Information Files 3–5.

FIGURE 1 Corn snake muscle anatomy and calculations. (a) Schematic showing a lateral view of the axial muscles of interest. For detailed anatomical drawings of the axial musculature of various snake species, see publications by Mosauer (1935) and Gasc (1967, 1974, 1981). (b) Transverse section of a contrast-enhanced μCT scan showing the muscles of interest. This particular scan shows the middle section of the 335 g snake. (c) Diagram showing our cross-product approach for calculating the potential relative contributions of each muscle to torque and its components (pitch, yaw, and roll). $\vec{r}$ represents the position vector running from the muscle to the condyle centroid (the point around which rotation occurs), and $\vec{F}$ represents the force vector running along the muscle's fibers between its two attachment points. We can measure $\vec{r}$ starting from either the medial or lateral attachment point of the muscle (A_m or A_L) or from the midpoint between the two attachments (A_c), which represent three different scenarios of snake movement: in the first two scenarios, the snake's body is anchored at either the anterior or posterior end, such that muscle contraction leads to movement of the opposite end toward the anchor point, and in the third scenario, neither end is anchored, such that both ends move towards each other. (d) Diagram showing the model for our approach that accounts for the changing curvature in a multiarticular system, relating snake epaxial muscle length $L_m(\kappa_v)$ to the curvature of the vertebral column (κ_v) in a way that can be generalized to other multiarticular systems. See Appendix 1 in Supplementary Materials and Methods for calculations and detailed explanation.

TABLE 1 Best estimate of medial and lateral attachment points for muscles of interest.

Muscle	Medial attachment	Lateral attachment
Semispinalis-spinalis	Centroid of anterior tendon bundle	Bottom corner of muscle
Multifidus	Top corner of muscle	Muscle centroid
Longissimus dorsi	Muscle centroid	Muscle centroid
Iliocostalis	Top corner/apex of muscle	Midpoint of bottom edge
Levator costae	Midpoint of top edge	Point nearest the rib

For one scan (the middle section of the 335 g individual), we obtained these anatomical data for five slices evenly spaced along a single vertebra situated near the middle of the scan. Then, we quantified intravertebral variation by calculating coefficients of variation and standard deviations for cross-sectional areas and muscle lever arms. We similarly quantified measurement error by digitizing a single one of those slices five times, calculating coefficients of variation and standard deviations for cross-sectional areas and muscle lever arms. Both intravertebral variation and measurement error were low (Supporting Information File 6). For the remaining scans (anterior, middle, and posterior region of each snake), we collected data for a single representative slice from a vertebra near the middle of the scan. We ensured homology by choosing slices where the posterior edge of the postzygapophysis could be located. This location is very near the vertebral condyle, which is functionally important because it is the point around which rotation happens.

2.3 | Muscle lever arms

We determined the relative contributions of each muscle to torque based on their lever arms (also called moment arms). This approach yields the expected motion at one attachment point of the muscle relative to the other attachment point, assuming that only one joint is moving. Torque is defined as the cross product $\vec{\tau} = \vec{r} \times \vec{F}$ (Figure 1c). The x, y, and z components of the torque vector represent contributions to dorsoventral flexion (pitch), lateral flexion (yaw), and torsion of the vertebral column (roll), respectively. $\vec{r}$ represents the position vector running from the muscle to the condyle centroid (the point around which rotation occurs), with $\vec{r_x}$ = the horizontal distance between the muscle and the condyle centroid, $\vec{r_y}$ = the vertical distance between the muscle and the condyle centroid, and $\vec{r_z} = 0$. $\vec{F}$ represents the force vector running along the muscle's fibers between its two attachment points, with $\vec{F_x}$ = the horizontal distance between the two muscle attachment points, $\vec{F_y}$ = the vertical distance between the two muscle attachment points, and $\vec{F_z}$ = the length of the muscle (number of vertebrae spanned times the length of one vertebra). Because we do not know how much force each muscle exerts, we converted each $\vec{F}$ to a unit vector ($\hat{F}$) by dividing all components by its magnitude ($\hat{F} = \frac{\vec{F}}{\|F\|}$). As a result, our output is not torque, but rather the muscles' lever arms (along with their x, y, and z components) in length units, which tell us how many N·m torque the muscles can produce per N force exerted. By our sign conventions, y and z (yaw and roll) components always have negative values, whereas x (pitch) components can have either positive or negative values. A positive pitch component indicates that the muscle flexes the vertebral column dorsally. A negative pitch component indicates ventral flexion.

We can measure $\vec{r}$ starting from either the medial or lateral attachment point of the muscle or from the midpoint between the two attachments, which represent three different scenarios of snake movement: in the first two scenarios, the snake's body is anchored at either the anterior or posterior end, such that muscle contraction leads to movement of the opposite end toward the anchor point, and in the third scenario, neither end is anchored, such that both ends move towards each other. We performed calculations for all three. However, note that the three calculations are the same for the longissimus dorsi because it runs horizontally along the body, not at an angle like the other muscles of interest. Thus, its anterior and posterior attachment points should be at the same location relative to the nearest condyle, and we therefore used the muscle centroid for both attachment points.

To assess how much the method for measuring the $\vec{r}$ vector mattered in our lever arm calculations, we calculated the standard deviation of the three measures for each region of a given muscle in a given snake (e.g., the standard deviation of three lever arms calculated for the semispinalis-spinalis from the anterior region of the 335 g snake, or the multifidus from the middle region of the 80 g snake, etc.) We repeated this process for the total magnitude of the vector and for the three individual components of the vectors.

We also used a more simplistic approach to estimate the potential relative contributions of each muscle to torque, computing the distance between each muscle centroid and the condyle centroid using the distance formula ($d_{\text{centroid}} = \sqrt{(x_1 - x_2)^2 + (y_1 - y_2)^2}$). This method omits most information about muscle architecture. However, if its results align reasonably well with the cross-product approach described above, then its simplicity and need for relatively few pieces of information could make it an attractive option for future studies requiring particularly large datasets and/or minimally-invasive data collection (e.g., if CT scanning is an option but dissections are not). We compared the simple distance approach to the cross-product approach with $\vec{r}$ measured from the midpoint between the muscles' anterior and posterior attachments, using their percent difference, calculated as $100 \times \frac{\text{simple distance} - \text{torque magnitude}}{\text{torque magnitude}}$.

Computations were performed in Python version 3.9.7. See Script 1 for the Python script, and File 7 for its output.

2.4 | Multiarticular approach to relating muscle length change with body posture

In addition to calculating muscle lever arms using simple mono-articular methods, we also employed a different approach to account

for the changing curvature in a multiarticular system. For this multiarticular approach, we related snake epaxial muscle length change to curvature change of the vertebral column in a way that can be generalized to other multiarticular systems. We did not apply this approach to the one hypaxial muscle in our study, the levator costae, because it spans only one joint. For multiarticular muscles, the curvature approach is more realistic than the cross-product approach in two ways: 1) lever arms change as posture changes (see Lieber & Boakes, 1988), a fact not accounted for in the cross-product approach; and 2) unlike the cross-product approach, this approach does not require the inaccurate assumption that only one joint is moving. The curvature approach relates changes in muscle length to changes in curvature (and thus joint angle) of the vertebral column. Because the sum of the mechanical work across all the intervertebral joints spanned must equal the total mechanical work done by the muscle, linking muscle length change to joint angle change allows calculation of torque.

For the curvature approach, we modeled the section of the vertebral column spanned by the muscle of interest as an arc of a circle (length = L_v) and the muscle as an arc of an Archimedean spiral (length at a given curvature = $L_m(\kappa_v)$; length when the body is straight $L_m(\kappa_v = 0) = L_v$; Figure 1d). We calculated L_v as the number of vertebrae spanned (determined by dissection) times the length of individual vertebrae (measured from μCT scans). The Archimedean spiral accounts for the fact that muscles do not necessarily run parallel to the vertebral column; for muscles that run at an angle, the anterior and posterior attachments are different distances from the axis of motion (e.g., as for the iliocostalis; Figure 1a). We put the equation for spiral arc length in terms of measurable anatomical values and vertebral column curvature (κ_v). See Appendix 1 in Supplementary Materials and Methods for detailed derivation.

We obtained the following equation for muscle length:

$$L_m(\kappa_v) = L_v - L_v\kappa_v\left(\frac{d_a + d_p}{2}\right) + \left(\frac{d_a - d_p}{2L_v\kappa_v}\right) (\ln(1 - \kappa_v d_p) - \ln(1 - \kappa_v d_a)) \quad (1)$$

where d_a and d_p equal the distances from the anterior and posterior ends of the muscle to the axis of motion (a line running through the vertebral condyles, in our system; Figure 1d). This distance is measured in the plane of motion (e.g., vertical distance from the axis of motion for bending in the dorsoventral plane, horizontal distance from the axis of motion for bending in the lateral plane).

The above equation has an interesting property: the term $L_v - L_v\kappa_v\left(\frac{d_a+d_p}{2}\right)$ represents an approximation of the muscle length at a given vertebral column curvature in which the muscle forms an arc displaced from the vertebral column by the mean of the anterior and posterior muscle attachment distances (d_a and d_p). The term $\left(\frac{d_a-d_p}{2L_v\kappa_v}\right)(\ln(1 - \kappa_v d_p) - \ln(1 - \kappa_v d_a))$ represents an adjustment for spirality, which accounts for the fact that the anterior and posterior attachments are at different distances from the axis of motion in muscles that do not run parallel to the vertebral column. Note that if the anterior and posterior ends of the muscle are the same distance from the vertebral column (i.e., $d_a = d_p$), then the spirality adjustment term becomes 0 and the equation gives the muscle length based on the formula for an arc.

For each of the muscles of interest, we used realistic values of L_v, d_a, and d_p to calculate expected muscle length for a series of curvature values ranging from 0 (the condition where the vertebral column is a straight line) to 0.175 mm^{-1} (see Appendix 2 in Supplementary Materials and Methods). We determined this value to be a reasonable maximum value for curvature by combining measured vertebral lengths in our study with Jurestovsky et al.'s (2020) observed values for maximal flexion between pairs of vertebrae (Appendix 2 in Supplementary Materials and Methods). To assess the importance of spirality in our system, we calculated the percent difference in muscle lengths calculated with and without the spirality adjustment, which 100 times the absolute value of the difference in calculated muscle lengths divided by their mean.

We can also consider the relationship between muscle length and curvature in terms of the absolute shortening of the muscle. Because the spirality adjustment in the previously derived equation made a negligible difference for all of the epaxial muscles under consideration (Results), we can assume that the muscle's resting length (when the vertebral column is straight) is equal to the length of vertebral column it spans (L_v). Thus, the absolute shortening of the muscle (S) is equal to the muscle's resting length minus its current length ($L_v - L_m(\kappa_v)$). Using the arc approximation part of the equation for $L_m(\kappa_v)$ given above, we can derive an equation relating absolute muscle shortening to curvature:

$$S = L_v - L_m(\kappa_v) = L_v\kappa_v\left(\frac{d_a + d_p}{2}\right) \quad (2)$$

The derivative of absolute muscle shortening (S) with respect to curvature (κ_v) equals:

$$\frac{dS}{d\kappa_v} = L_v\left(\frac{d_a + d_p}{2}\right) \quad (3)$$

Using geometry, we can relate curvature to intervertebral joint angle as $\kappa_v \approx \frac{\varnothing}{L_i}$, where L_i equals the length of each vertebra and $\varnothing$ equals the angle between each pair of vertebrae in radians, (Appendix 2 in Supplementary Materials and Methods). Substituting $\frac{\varnothing}{L_i}$ for κ_v, we can put S in terms of $\varnothing$ instead of κ_v:

$$S = L_v - L_m(\kappa_v) = L_v\frac{\varnothing}{L_i}\left(\frac{d_a + d_p}{2}\right) \quad (4)$$

The length of vertebral column spanned by the muscle of interest (L_v) divided by the length of an individual vertebra (L_i) equals the number of vertebrae spanned by the muscle, N_v, so we can also put S in terms of the number of vertebrae spanned and the angles between them:

$$S = N_v \varnothing \left(\frac{d_a + d_p}{2} \right) \quad (5)$$

The derivative of absolute muscle shortening (S) with respect to the angle between the vertebrae ($\varnothing$) equals:

$$\frac{dS}{d\varnothing} = N_v \left(\frac{d_a + d_p}{2} \right) \quad (6)$$

For the case of a muscle spanning a single joint ($N_v = 1$), $\frac{dS}{d\varnothing}$ converges on the simple lever arm, supporting the validity of our approach.

2.5 | Statistical analyses

We tested for effects of snake mass, body region (anterior, middle, posterior), and their interaction on vertebral length using analysis of covariance (ANCOVA) with Type III sums of squares (package *car*, R 4.2.1; Fox & Weisberg, 2019; R Core Team, 2022). Before the ANCOVA, we log-transformed mass and vertebral length, and averaged the lengths of 6-9 vertebrae measured in each scan. The interaction was not significant, so we dropped it for the final model. We also used ANCOVA to examine whether muscle cross-sectional area was predicted by snake mass, body region (anterior, middle, and posterior), and/or muscle type (five muscles), also log-transforming values before the analysis. We initially included all two-way interactions in the ANCOVA models for muscle cross-sectional area, but then dropped the interactions that were not significant.

We also used ANCOVA with Type III sums of squares to examine the effect of snake mass, body region (anterior, middle, posterior), and muscle identity (five muscles) on total magnitude of lever arm and its three components (pitch, yaw, and roll) (package *car*, R 4.2.1; Fox & Weisberg, 2019; R Core Team, 2022). We initially included all two-way interactions in these ANCOVA models, but then dropped the interactions that were not significant. For this analysis, we used the torque calculations where the $\vec{r}$ vector was measured from the midpoint between the medial and lateral attachments.

To examine scaling of anatomy and lever arms with body size, we conducted reduced major axis (RMA) regression of each $\log_{10}$-transformed trait on $\log_{10}$ mass, using data from the middle section of each snake. As with the ANCOVA, we conducted the analysis of vertebral length using average value for each snake section, and for lever arms we used the torque calculations where the $\vec{r}$ vector was measured from the midpoint between the medial and lateral attachments. Because lever arm calculations required an arbitrary decision of sign convention that led to negative values for pitch components in some muscles (those that flex the vertebral column ventrally), and negative values for yaw and roll components in all muscles, we took the absolute value before log transforming and running RMA analyses. Under isometry (geometric similarity), vertebral length would be expected to have a slope of $\frac{1}{3}$ and all cross-sectional areas would be expected to have a slope of $\frac{2}{3}$. Since lever arms are linear distances, they would be expected to have a slope of $\frac{1}{3}$. We calculated confidence intervals for the estimated RMA slopes to determine whether they included the expectation under isometry.

3 | RESULTS

3.1 | Muscle spans

We determined the number of vertebrae spanned in a 510 g specimen for the semispinalis-spinalis, the multifidus, the longissimus dorsi, the iliocostalis, and the levator costae (Figure 1a). The semispinalis-spinalis spanned 19 total vertebrae, with the anterior tendon spanning 11, the spinalis muscle body spanning 4–5 (because the posterior attachment was spread across two vertebrae), the semispinalis muscle body spanning seven, and the posterior tendon spanning one vertebra. The spinalis and semispinalis muscle bodies were joined for three vertebrae behind the tendon before splitting, so we counted those three vertebrae as part of the span for both of them, plus an additional 1–2 for the spinalis and an additional four for the semispinalis. The multifidus spanned three vertebrae, with muscle body representing about half its length and posterior tendon representing the other half. The longissimus dorsi spanned nine total vertebrae, with dorsal anterior tendon spanning two, ventral anterior tendon spanning one, and muscle body spanning seven vertebrae. The iliocostalis spanned 16 total vertebrae, with anterior tendon spanning four, anterior muscle body spanning five, middle tendon spanning one, posterior muscle body spanning five, and posterior tendon spanning one vertebra. The levator costae spanned a single vertebra.

3.2 | Anatomy: Influence of snake size and body region

Vertebral length increased significantly with snake mass and did not vary among body regions (Tables 2 and 3). The cross-sectional areas of muscles increased significantly with snake mass and varied among regions (Table 2), with higher cross-sectional areas in the anterior-most snake sections scanned than in the middle ones (Table 3). There was a significant interaction between mass and region (Table 2), and muscle identity was also significantly related to cross-sectional area (Table 2), with the levator costae having significantly lower cross-sectional area than other muscles (Table 3).

Vertebral length scaled isometrically with snake mass, whereas all muscle cross-sectional areas had estimated slopes higher than the expectation under isometry, with confidence intervals for three of the five muscles excluding the expectation under isometry (Table 4, Figure 2).

3.3 | Lever arms: Comparison of different calculation methods

The cross-product calculations of lever arm with three different methods for measuring the $\vec{r}$ vector (starting from the medial attachment, from the

TABLE 2 Results from the ANCOVA analyses.

		Sums of squares	*df*	*F*	*p*
Log_{10} vertebral length (mm)	Intercept	0.002	1	1.481	.244
	Log mass (g)	**0.120**	**1**	**102.873**	**7.8E-08**
	Snake region	**0.007**	**2**	**3.091**	**.077**
	Residuals	0.016	14	-	-
Log_{10} muscle cross-sectional area (mm^2)	Intercept	1.332	1	153.615	<2.2e-16
	Log mass (g)	**2.397**	**1**	**276.490**	**<2.2e-16**
	Snake region	**0.096**	**2**	**5.529**	**.006**
	Muscle	**0.289**	**4**	**8.333**	**1.1E-05**
	Log mass × snake region	**0.079**	**2**	**4.539**	**.014**
	Residuals	0.694	80	-	-
Lever arms total magnitude	Intercept	180.988	1	587.143	3.9E-39
	Log mass (g)	**84.945**	**1**	**275.571**	**6.0E-28**
	Snake region	**7.226**	**2**	**11.721**	**3.3E-05**
	Muscle	**62.911**	**4**	**51.023**	**1.7E-21**
	Residuals	25.277	82	-	-
Lever arms pitch component	Intercept	0.110	1	1.141	.289
	Log mass (g)	**0.488**	**1**	**5.058**	**.027**
	Snake region	**3.410**	**2**	**17.677**	**4.7E-07**
	Muscle	**24.211**	**4**	**62.746**	**1.3E-23**
	Log mass × muscle	**19.178**	**4**	**49.704**	**1.0E-20**
	Residuals	7.524	78	-	-
Lever arms yaw component	Intercept	61.321	1	239.634	1.7E-25
	Log mass (g)	**26.741**	**1**	**104.500**	**4.7E-16**
	Snake region	**3.622**	**2**	**7.076**	**1.5E-03**
	Muscle	**28.049**	**4**	**27.403**	**3.2E-14**
	Log mass × muscle	**13.782**	**4**	**13.465**	**2.2E-08**
	Residuals	19.960	78	-	-
Lever arms roll component	Intercept	0.131	1	4.127	.046
	Log mass (g)	**0.187**	**1**	**5.871**	**.018**
	Snake region	**0.110**	**2**	**1.736**	**1.8E-01**
	Muscle	**2.230**	**4**	**17.534**	**2.7E-10**
	Log mass × muscle	**1.074**	**4**	**8.442**	**1.0E-05**
	Residuals	2.480	78	-	-

Note: Bold text indicates significant results. For vertebral length, we tested for effects of snake mass, body region (anterior, middle, posterior), or their interaction. Before the ANCOVA, we log-transformed mass and vertebral length, and averaged the lengths of 6-9 vertebrae measured in each scan. For muscle cross-sectional area and muscle lever arms, we tested for effects of snake mass, body region (anterior, middle, posterior), muscle (five muscles) or two-way interactions, log-transforming values before the analysis. In all cases, if any interactions were not significant, we re-ran the ANCOVA without them.

Abbreviation: ANCOVA, analysis of covariance.

TABLE 3 Estimated partial coefficients and their 95% confidence intervals from the ANCOVA analyses of vertebral length and muscle cross-sectional area.

			Estimated partial coefficient	CI, lower	CI, upper	Std. Error	*t* value	*p* value
Log vertebral length (mm)	Intercept	-	−0.077	−0.211	0.057	0.062	−1.237	.236
	Log mass (g)	**-**	**0.286**	**0.226**	**0.346**	**0.028**	**10.143**	**7.8E-08**
	Snake region	Anterior	0.001	−0.041	0.044	0.020	0.063	.951
		Posterior	**−0.042**	**−0.084**	**0.000**	**0.020**	**−2.121**	**.052**
Log muscle cross-sectional area (mm^2)	Intercept	-	−1.620	−1.880	−1.360	0.131	−12.394	2.6E-20
	Log mass (g)	**-**	**0.988**	**0.870**	**1.106**	**0.059**	**16.628**	**1.1E-27**
	Snake region	**Anterior**	**0.514**	**0.150**	**0.877**	**0.183**	**2.811**	**.006**
		Posterior	−0.024	−0.388	0.339	0.183	−0.134	.894
	Muscle	Semispinalis-spinalis	−0.030	−0.092	0.032	0.031	−0.961	.339
		Multifidus	−0.053	−0.114	0.009	0.031	−1.696	.094
		Iliocostalis	0.016	−0.046	0.078	0.031	0.523	.602
		Levator costae	**−0.145**	**−0.207**	**−0.083**	**0.031**	**−4.676**	**1.2E-05**
	Log mass × snake region	**Log mass × anterior**	**−0.246**	**−0.414**	**−0.079**	**0.084**	**−2.930**	**.004**
		Log mass × posterior	−0.072	−0.239	0.095	0.084	−0.859	.393
Lever arms total magnitude	Intercept	-	3.143	2.774	3.512	0.185	16.955	1.6E-28
	Log mass (g)	**-**	**0.010**	**0.009**	**0.011**	**0.001**	**16.600**	**6.0E-28**
	Snake region	Anterior	0.079	−0.206	0.364	0.143	0.551	.583
		Posterior	**−0.558**	**−0.843**	**−0.272**	**0.143**	**−3.890**	**2.0E-04**
	Log mass × muscle	**Semispinalis-spinalis**	**−0.739**	**−1.108**	**−0.371**	**0.185**	**−3.996**	**1.4E-04**
		Multifidus	**−1.203**	**−1.571**	**−0.835**	**0.185**	**−6.502**	**5.8E-09**
		Iliocostalis	**1.270**	**0.902**	**1.638**	**0.185**	**6.862**	**1.2E-09**
		Levator costae	−0.142	−0.510	0.226	0.185	−0.768	.444
Lever arms pitch component	Intercept	-	0.991	0.684	1.297	0.154	6.425	9.6E-09
	Log mass (g)	**-**	**0.004**	**0.003**	**0.006**	**0.001**	**5.948**	**7.3E-08**
	Snake region	**Anterior**	**0.336**	**0.176**	**0.496**	**0.080**	**4.190**	**7.3E-05**
		Posterior	−0.125	−0.285	0.035	0.080	−1.559	.123
	Muscle	**Semispinalis-spinalis**	**0.988**	**0.574**	**1.402**	**0.208**	**4.752**	**9.0E-06**
		Multifidus	**0.799**	**0.385**	**1.213**	**0.208**	**3.842**	**2.5E-04**
		Iliocostalis	**−1.162**	**−1.576**	**−0.748**	**0.208**	**−5.587**	**3.3E-07**
		Levator costae	**−1.633**	**−2.047**	**−1.219**	**0.208**	**−7.850**	**1.8E-11**
	Log mass × muscle	**Log mass × semispinalis-spinalis**	**0.004**	**0.002**	**0.006**	**0.001**	**3.777**	**3.1E-04**
		Log mass × multifidus	**0.004**	**0.002**	**0.006**	**0.001**	**3.675**	**4.3E-04**
		Log mass × iliocostalis	**−0.006**	**−0.008**	**−0.004**	**0.001**	**−5.796**	**1.4E-07**
		Log mass × levator costae	**−0.007**	**−0.009**	**−0.005**	**0.001**	**−6.544**	**5.7E-09**
Lever arms yaw component	Intercept	-	−2.877	−3.377	−2.377	0.251	−11.457	2.2E-18
	Log mass (g)	**-**	**−0.009**	**−0.012**	**−0.007**	**0.001**	**−7.711**	**3.4E-11**
	Snake region	Anterior	0.081	−0.179	0.341	0.131	0.623	.535

(Continues)

TABLE 3 (Continued)

			Estimated partial coefficient	CI, lower	CI, upper	Std. Error	*t* value	*p* value
		Posterior	**0.460**	**0.200**	**0.720**	**0.131**	**3.524**	**.001**
	Muscle	**Semispinalis-spinalis**	**1.482**	**0.807**	**2.156**	**0.339**	**4.375**	**3.7E-05**
		Multifidus	**1.982**	**1.308**	**2.657**	**0.339**	**5.852**	**1.1E-07**
		Iliocostalis	**−1.092**	**−1.766**	**−0.417**	**0.339**	**−3.223**	**.002**
		Levator costae	−0.094	−0.769	0.580	0.339	−0.278	.782
	Log mass × muscle	**Log mass × semispinalis-spinalis**	**0.006**	**0.002**	**0.009**	**0.002**	**3.453**	**.001**
		Log mass × multifidus	**0.008**	**0.004**	**0.011**	**0.002**	**4.603**	**1.6E-05**
		Log mass × iliocostalis	−0.003	−0.006	0.000	0.002	−1.776	.080
		Log mass × levator costae	0.001	−0.002	0.005	0.002	0.761	.449
Lever arms roll component	Intercept	-	−0.016	−0.192	0.160	0.089	−0.178	.859
	Log mass (g)	-	0.000	−0.001	0.001	0.000	0.000	1.000
	Snake region	Anterior	−0.017	−0.109	0.075	0.046	−0.369	.713
		Posterior	0.064	−0.027	0.156	0.046	1.397	.166
	Muscle	Semispinalis-spinalis	−0.099	−0.336	0.139	0.119	−0.826	.412
		Multifidus	**−0.312**	**−0.550**	**−0.074**	**0.119**	**−2.614**	**.011**
		Iliocostalis	−0.147	−0.385	0.091	0.119	−1.231	.222
		Levator costae	**−0.889**	**−1.126**	**−0.651**	**0.119**	**−7.442**	**1.1E-10**
	Log mass × muscle	Log mass × semispinalis-spinalis	−0.001	−0.002	0.001	0.001	−0.969	.336
		Log mass × multifidus	**−0.001**	**−0.003**	**0.000**	**0.001**	**−2.491**	**.015**
		Log mass × iliocostalis	−0.001	−0.002	0.000	0.001	−1.713	.091
		Log mass × levator costae	**−0.003**	**−0.004**	**−0.002**	**0.001**	**−5.400**	**7.0E-07**

Note: The final model for vertebral length was log mass (continuous covariate) + snake region (anterior, middle, posterior). The final model for muscle cross-sectional area was log mass (continuous covariate) + snake region (anterior, middle, posterior) + muscle (semispinalis-spinalis, multifidus, longissimus dorsi, iliocostalis, levator costae) + log mass * snake region. For categorical variables, one category serves as the baseline against which other categories are compared, and therefore does not have a row in the table. "Middle" is the base category for snake region, and "longissimus dorsi" is the base category for muscle.

Abbreviations: ANCOVA, analysis of covariance; CI, confidence interval.

lateral attachment, or from the midpoint of the two) did not produce substantially different results (Figure 3). For the lever arm vectors' total magnitude, the standard deviations were generally less than 0.001 m (i.e., less than 0.001 N·m torque per N force). For dorsoventral flexion (pitch), the method for calculating $\vec{r}$ had the greatest effect on the iliocostalis, with standard deviations ranging from 0.0015 to 0.0026 m in the two largest specimens, and on the semispinalis-spinalis, with standard deviations ranging from 0.0008 to 0.0015 m in the two largest specimens. For lateral flexion (yaw), the method for calculating $\vec{r}$ had the greatest effect on the semispinalis-spinalis, with standard deviations ranging from 0.0015 to 0.0021 m in the two largest specimens. The method for calculating $\vec{r}$ had no effect on roll.

The simple distance approach for estimating lever arms differed only slightly from the cross-product approach with $\vec{r}$ measured from the midpoint between the muscles' anterior and posterior attachments (Figure 3; Supporting Information File S6). On average, the simple distance approach yielded a value 0.04% higher than the cross-product approach, ranging from 9.4% lower to 17.6% higher, with 58 of the 90 calculations (64.4%) within ± 5%. Only the levator costae had simple distance approximations that differed from the lever arm calculation by more than ± 10%, with simple distance sometimes underestimating and sometimes overestimating the lever arm calculation. Simple distance consistently produced lower values for the multifidus (average 5.8% lower than lever arm) and higher values for the semispinalis-spinalis (average 5.7% higher than lever arm) than did lever arm calculations. The two approaches yielded nearly the same values for the iliocostalis (simple distance averaged 1.4% lower) and the exact same values for the longissimus dorsi.

TABLE 4 Results from the reduced major axis (RMA) analysis of scaling for vertebral length, muscle cross-sectional areas, and muscle lever arms.

		r^2	p	RMA intercept	RMA slope	RMA CI lower	RMA CI upper	Expectation under isometry	Departure from isometry?
Length	Vertebrae	0.904	.004	−0.111	0.301	0.198	0.458	0.333	
Cross-sectional area	**Semispinalis-spinalis**	**0.923**	**.002**	**−1.626**	**0.971**	**0.667**	**1.415**	**0.667**	**+ allometry**
	Multifidus	0.906	.003	−1.668	0.987	0.652	1.493	0.667	
	Longissimus dorsi	0.899	.004	−1.527	0.944	0.616	1.448	0.667	
	Iliocostalis	**0.934**	**.002**	**−1.702**	**1.032**	**0.728**	**1.462**	**0.667**	**+ allometry**
	Levator costae	**0.885**	**.005**	**−2.313**	**1.250**	**0.793**	**1.972**	**0.667**	**+ allometry**
Lever arm total magnitude	Semispinalis-spinalis	0.925	.002	−0.167	0.354	0.244	0.513	0.333	
	Multifidus	0.907	.003	−0.268	0.375	0.248	0.566	0.333	
	Longissimus dorsi	0.962	.001	−0.121	0.371	0.284	0.484	0.333	
	Iliocostalis	0.917	.003	−0.051	0.386	0.262	0.571	0.333	
	Levator costae	0.733	.030	−0.156	0.373	0.191	0.727	0.333	
Pitch component	Semispinalis-spinalis	0.879	.006	−0.305	0.389	0.244	0.619	0.333	
	Multifidus	0.900	.004	−0.329	0.389	0.254	0.595	0.333	
	Longissimus dorsi	0.758	.024	−0.849	0.493	0.260	0.933	0.333	
	Iliocostalis	**0.723**	**.032**	**−2.186**	**0.882**	**0.448**	**1.736**	**0.333**	**+ allometry**
	Levator costae	0.718	.033	−1.149	0.544	0.275	1.076	0.333	
Yaw component	Semispinalis-spinalis	0.923	.002	−0.310	0.278	0.190	0.405	0.333	
	Multifidus	0.752	.025	−0.578	0.285	0.150	0.544	0.333	
	Longissimus dorsi	0.959	.001	−0.134	0.364	0.275	0.480	0.333	
	Iliocostalis	0.915	.003	−0.045	0.382	0.257	0.568	0.333	
	Levator costae	0.697	.039	−0.131	0.344	0.170	0.696	0.333	
Roll component	**Semispinalis-spinalis**	**0.939**	**.001**	**−1.749**	**0.492**	**0.351**	**0.687**	**0.333**	**+ allometry**
	Multifidus	0.833	.011	−1.300	0.497	0.289	0.852	0.333	
	Longissimus dorsi	-	-	-	-	-	-	-	
	Iliocostalis	**0.779**	**.020**	**−1.821**	**0.615**	**0.333**	**1.137**	**0.333**	**+ allometry**
	Levator costae	**0.616**	**.064**	**−1.458**	**0.729**	**0.334**	**1.588**	**0.333**	**+ allometry**

Note: Analyses were conducted using log10-transformed traits, measured from the middle section of each snake ($n = 6$). Traits that depart significantly from isometry (based on their confidence intervals not crossing the expectation under isometry) are indicated in bold.

Abbreviation: CI, confidence interval.

3.4 | Lever arms: Influence of snake size, muscle, and body region

Mass, snake region, and muscle significantly influenced lever arm total magnitudes and their individual components. We found a significant interaction of mass and muscle for the individual components, but not for total magnitude (Table 2; Figure 3). Lever arm total magnitude is significantly lower in the posterior region, whereas lever arm components differ in which region has higher values (Table 3; Figure 3). The iliocostalis has the greatest total lever arm (Table 3; Figure 3).

We must remember sign conventions in interpreting the ANCOVA results for individual lever arm components. The pitch (dorsoventral flexion) component can be either positive or negative, with the former indicating that a muscle causes dorsal flexion and the latter indicating ventral flexion. The semispinalis-spinalis, multifidus,

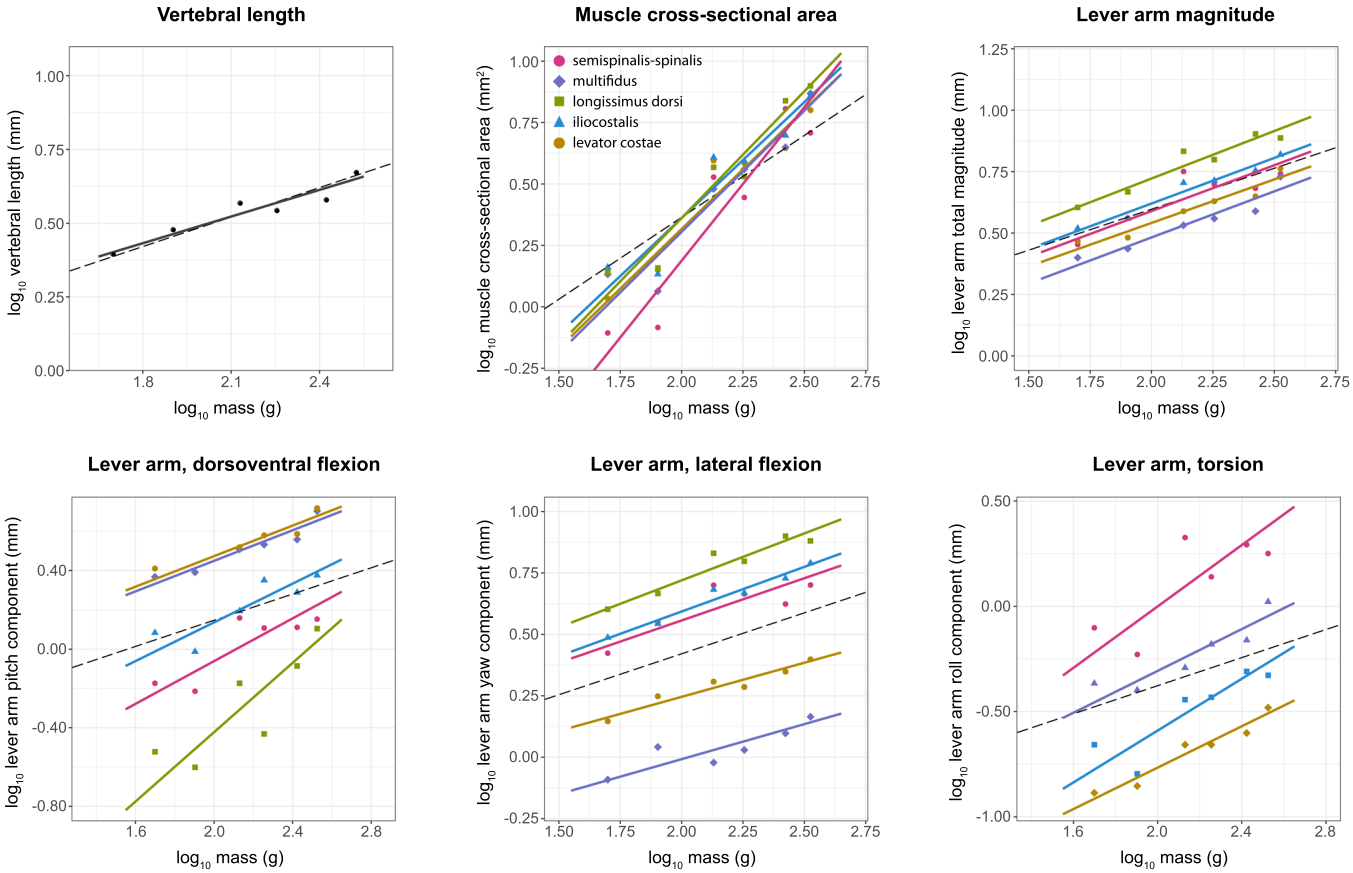

FIGURE 2 Scaling of vertebral length, muscle cross-sectional areas, and muscle lever arms with mass. We conducted reduced major axis (RMA) analyses using $\log_{10}$-transformed traits, measured from the middle section of each snake ($n = 6$). Dashed lines represent the expectation under isometry, and solid line segments represent the RMA estimated slopes. The legend shown in the muscle cross-sectional area plot also applies to the four lever arm plots. Note that the longissimus dorsi does not contribute to roll.

and longissimus dorsi can all contribute to dorsal flexion when they contract, with the semispinalis-spinalis and multifidus having about twice the lever arm pitch (x) component of the longissimus dorsi; the iliocostalis and the levator costae both potentially contribute to ventral flexion (Table 3; Figure 3). However, note that the iliocostalis has positive values for pitch when torque is calculated with $\vec{r}$ measured from the medial muscle attachment, the only case where the choice of $\vec{r}$ measurement changes the predicted direction of flexion (Figure 3). The lever arm components for yaw (lateral flexion) and roll (torsion) always have negative values, so significantly lower values for those components counterintuitively indicate greater contributions to those movements.

The iliocostalis contributes significantly more to lateral flexion than does the longissimus dorsi (the muscle used as the base category for comparisons), while the semispinalis-spinalis and the multifidus contribute significantly less to lateral flexion (Table 3; Figure 3). The multifidus and the levator costae can contribute significantly more to roll than can the other muscles, although the roll components of all muscles' lever arms are generally quite low compared to pitch and yaw (Table 3; Figure 3). The results of ANCOVA analyses for pitch (dorsoventral flexion), yaw (lateral flexion), and roll (torsion) all show a significant interaction between muscle (a categorical variable) and mass (the continuous covariate), which means we must use caution in attempting to interpret exactly how much each muscle contributes to a given lever arm component. Although a given muscle may generally make a greater contribution to a given component of lever arm, its relative contribution is not the same for all snake sizes. To illustrate this point: for yaw (lateral flexion), the semispinalis-spinalis has an estimated partial coefficient of approximately 1.5 when compared to the longissimus dorsi (Table 3), but a significant muscle*mass interaction means the semispinalis-spinalis lever arm yaw component is not 1.5 times that of the longissimus dorsi in every size snake; it might be higher than 1.5 at one end of the size range, and lower than 1.5 at the other end of the size range.

The scaling coefficients for lever arm total magnitudes did not deviate from the expectations under isometry, and r^2 values were generally high for epaxial muscles (Table 4, Figure 2). Most of the individual lever arm components also scaled isometrically, with the exception of significant positive allometry for the pitch component of the iliocostalis, and significant positive allometry in the roll components of the semispinalis-spinalis, the iliocostalis, and the levator costae (Table 4, Figure 2). The r^2 values for the individual lever arm

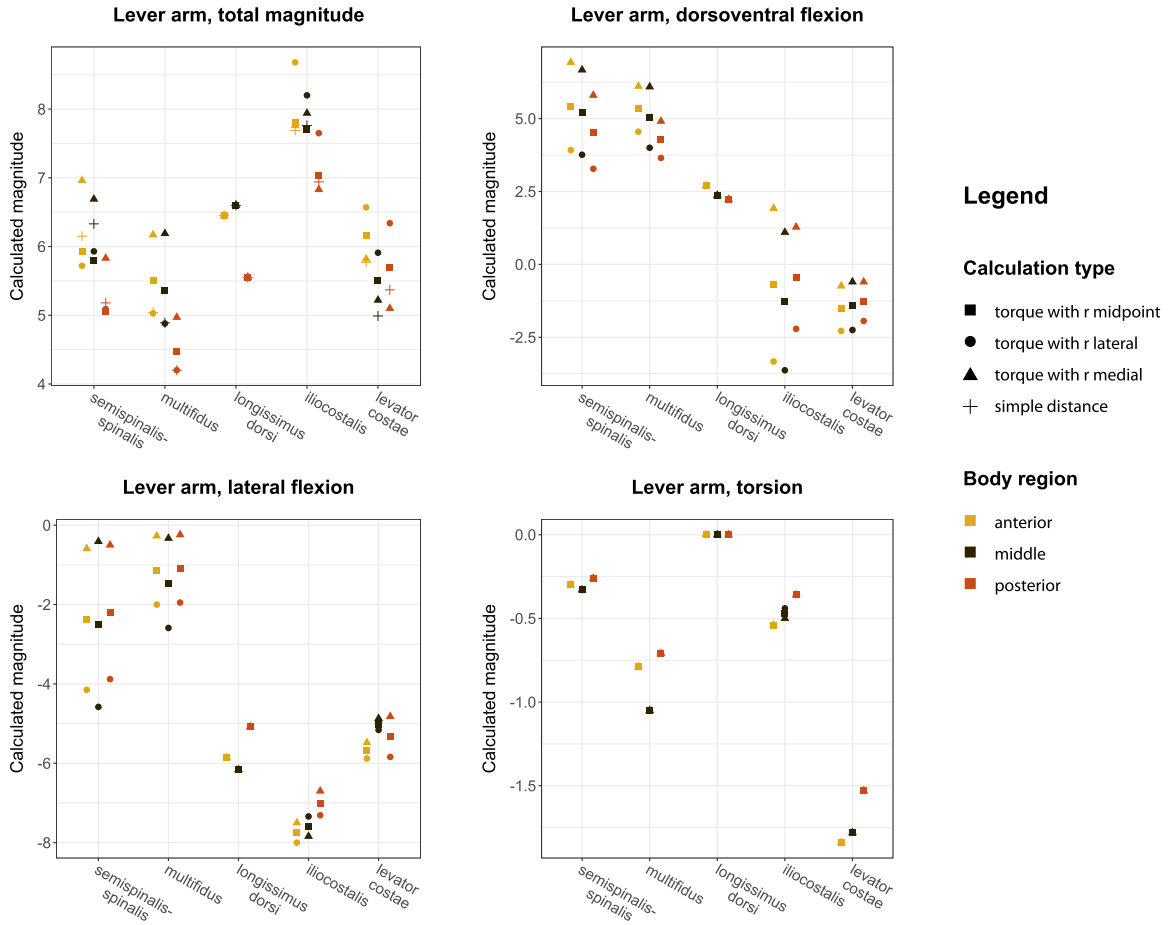

FIGURE 3 Comparison of lever arms across different muscles for the total magnitude, pitch component (dorsoventral flexion), yaw component (lateral flexion), and roll (torsion). Data from the 335 g snake. Symbol shapes indicate different methods for measuring the $\vec{r}$ vector (starting from the lateral attachment, from the medial attachment, or from the midpoint of the two). Note that simple distance (symbol shaped like a "+") appears only in the total magnitude panel. Symbol colors indicate the region of the body (anterior, middle, posterior).

components for various muscles showed more variability than did r^2 values for lever arm total magnitude or muscle cross-sectional area (Table 4).

3.5 | Curvature calculations

We found that the spirality adjustment term in Equation (1) made a negligible difference over simply using the arc approximation term for all of the epaxial muscles under consideration: the calculated muscle lengths with and without the spirality adjustment were always within 0.5% of each other.

For the epaxial muscles under consideration, a graph of intervertebral angle versus muscle shortening for dorsoventral flexion (Figure 4) clearly shows that the semispinalis-spinalis, multifidus, and longissimus dorsi act as dorsal flexors (as indicated by their positive slopes, given our sign convention), whereas the iliocostalis acts as a ventral flexor (as indicated by its negative slope). Steeper slopes indicate that a given % change in muscle length leads to more motion (a greater change in curvature), but less torque. The longissimus dorsi must shorten by approximately 6%–12% of its total resting length to produce intervertebral angles of approximately 11° (a reasonable maximum for dorsal flexion based on Jurestovsky et al., 2020), whereas semispinalis-spinalis and multifidus must shorten by approximately 20%–25% of their total resting length to achieve the same result. Therefore, the longissimus should reach maximum curvature about twice as quickly as the latter two muscles. Due to the trade-off with mechanical advantage, the semispinalis-spinalis and multifidus should produce about twice as much torque for a given amount of relative shortening, aligning with the cross-product results for lever arm pitch (x) component (Table 3; Figure 3). The iliocostalis must shorten by only approximately 2%–8% of its total resting length to produce intervertebral angles of approximately 16° during ventral flexion (a reasonable maximum based on Jurestovsky et al., 2020), suggesting it produces fast rather than forceful body motion.

Equation (5) serves to link absolute muscle length change (S) to joint angle change ($\varnothing$). This equation shows that that increasing multiarticular span (N_v) results in smaller joint angle changes ($\varnothing$) spread across more joints (N_v). Thus, for muscles spanning more joints, a given absolute muscle length change (S) does not change the joint angles (and therefore curvature) as much as does the same absolute muscle length change in a shorter muscle.

When considered in terms of mechanical work, the sum of the work done across all the joints must equal the work done by the

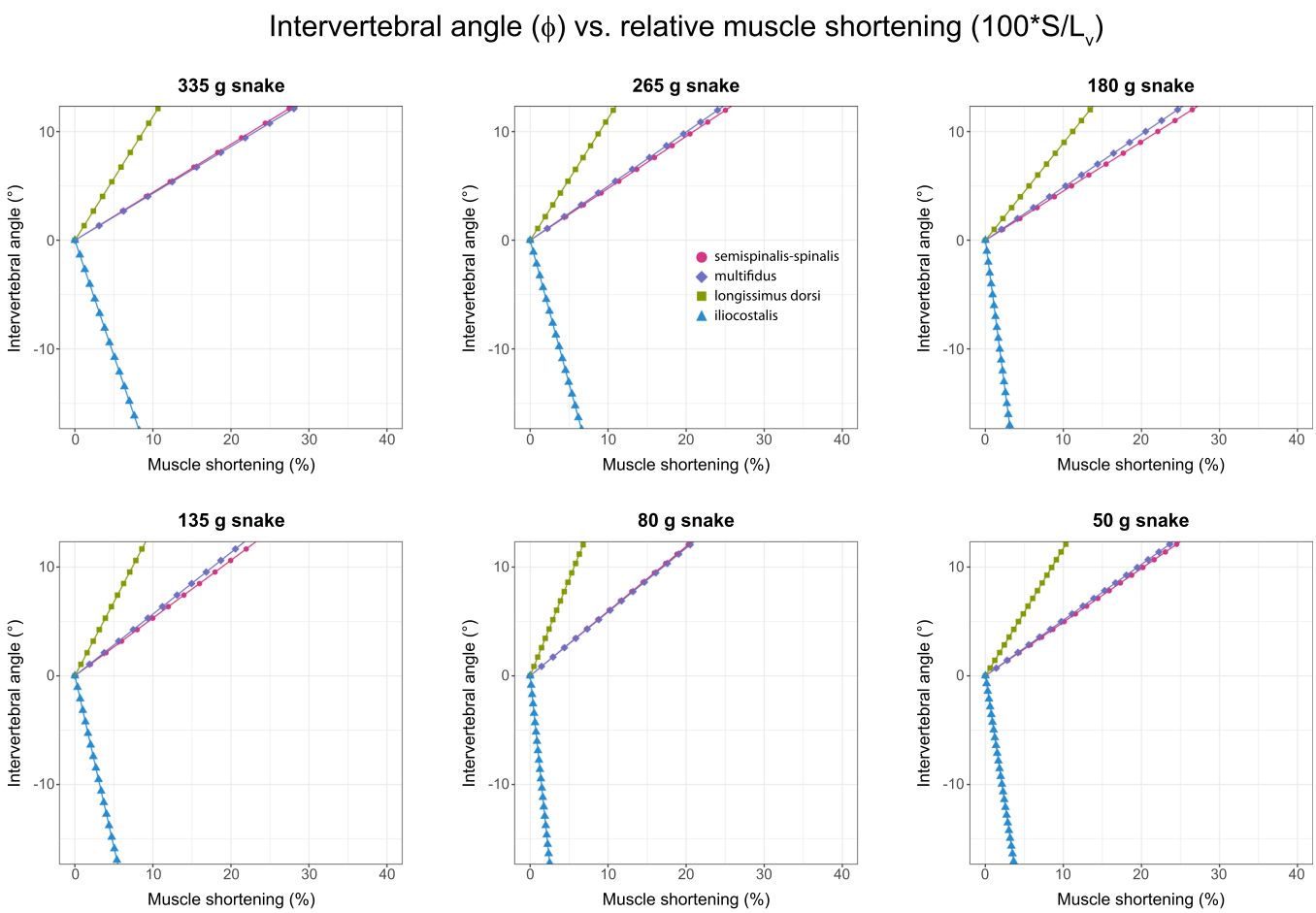

FIGURE 4 Plots of intervertebral angle versus relative muscle shortening during dorsoventral flexion for all four epaxial muscles in the six differently-sized snakes that we examined. The legend shown in the top middle plot applies to all six plots. Absolute muscle shortening (S) was calculated for a range of intervertebral angles ($\varnothing$) using Equation (4). The Python code used for calculations can be found in Supplemental Materials and Methods, Script 2. We divided absolute muscle shortening by each muscle's resting length (L_v) and multiplied by 100 to get relative muscle shortening as a % of the resting length. Due to our sign convention for d_a and d_p, positive intervertebral angles indicate dorsal flexion, whereas negative intervertebral angles indicate ventral flexion. Steeper slopes indicate that a given % change in muscle length leads to more motion (a greater change in curvature), but less torque. The y-axis ranges from −16° to 11° based on data for maximum intervertebral angles during ventral and dorsal flexion in corn snakes (Jurestovsky et al., 2020).

muscle. Thus, for a muscle exerting a constant force (F) as it shortens, we can multiply Equation (5) by F, which equates to the summed work across all the joints:

$$FS = FN_v\varnothing\left(\frac{d_a + d_p}{2}\right) = \sum_i^{N_v} \tau_i\varnothing_i \tag{7}$$

If curvature is constant along the vertebral column, then joint angle ($\varnothing$) between each pair of vertebrae must also be constant. Since the force (F) is also constant along the length of a single muscle, and the lever arm ($\frac{d_a+d_p}{2}$) is constant in the arc approximation, then the torque must also be constant across all joints. Thus, from the summation identity for constants,

$$FN_v\varnothing\left(\frac{d_a + d_p}{2}\right) = N_v\varnothing \quad \tau \tag{8}$$

which simplifies to

$$F\left(\frac{d_a + d_p}{2}\right) = \tau \tag{9}$$

This equation shows that the multiarticular method yields lever arm values identical to the average distance of the attachment points from the vertebral joints, under certain assumptions.

4 | DISCUSSION

4.1 | Basic anatomy

Muscle spans in *P. guttatus* generally resembled those of its congener *P. obsoletus* and other closely related species (Jayne, 1982, 1988b; Penning, 2018; Tingle et al., 2017). The epaxial muscle cross-sectional

areas did not significantly differ from each other within the roughly mid-body section of *P. guttatus* that we dissected (Table 3), which means any differences in their torque-generating capabilities would depend instead on length and orientation. Jayne and Riley (2007) similarly found that the semispinalis-spinalis, multifidus, longissimus dorsi, and iliocostalis had approximately the same cross-sectional areas at mid-body for the brown tree snake *Boiga irregularis*; however, closer to the head (at ~10% SVL), the iliocostalis had relatively more cross-sectional area and the longissimus dorsi had relatively less. Thus, for some species, one might expect regional differences in whether cross-sectional area is a major contributor to differences in torque-generating capabilities of epaxial muscles.

In addition to the muscles included in the present analysis, our CT scans showed a region of tissue bounded dorsally by the longissimus dorsi and ventrally by the levator costae, consistent with the location of the poorly known interarticularis superior and interarticularis inferior (Gasc, 1981). Due to the indistinctness of this area of tissue, and therefore the impossibility of separately digitizing the two interarticularis muscles, we were unable to include them in our analysis. However, this section of tissue represented appreciable cross-sectional area, ranging from 15% to 30% the combined area of all five muscles considered in this present study. Therefore, it would be worthwhile for future studies to study the potential role of these deeper muscles in force production.

4.2 | Regional variation of anatomy and lever arms

We found evidence for regional variation in anatomy, including shorter vertebrae in the posterior-most section of the body and larger muscle cross-sectional areas in the anterior-most section measured (Tables 2 and 3). A significant interaction between mass and body region in the ANCOVA model for muscle cross-sectional area complicates our interpretation of the significant main effect of region. This interaction indicates snakes of different sizes in our sample show different patterns of regionalization. Although snake bodies appear relatively uniform along their longitudinal axis compared to the bodies of tetrapods with fore- and hindlimbs attached to pectoral and pelvic girdles, previous studies have shown several ways the axial musculoskeletal system can vary along the length of a snake. Some species have conspicuous regional adaptations, like the presence of shell-cracking hypapophyses on some vertebrae in egg-eating snakes or specializations associated with hooding behavior in cobras (Gans, 1974; Young & Kardong, 2010). Other species show more subtle longitudinal differences in size or shape of morphological features (Lourdais et al., 2005; Nicodemo, 2012; Sherratt & Coutts, Rasmussen, et al., 2019; Sherratt & Sanders, 2020).

Longitudinal gradients in the vertebrae, ribs, muscles, and/or tendons could have functional consequences for behaviors involving all or part of the body, and merit further investigation. We did find that lever arm total magnitude and the value of all components differed significantly among body regions, highlighting the existence of functional differences along the body (Tables 2 and 3; Figure 3). However, our study is not primarily focused on regional variation, and our results do not provide a detailed picture of the causes and consequences of regional functional variation. Future studies with broader sampling of species, sizes, and body regions could further explore the regionalization of musculo-skeletal anatomy, the consequences of regionalization for function, and how regionalization might change over ontogeny.

4.3 | Scaling of anatomy and lever arms

The scaling of an organism's parts with its overall size can profoundly affect function. In corn snakes, vertebral length and most lever arms do not significantly depart from isometry (Table 4; Figure 2). Muscle cross-sectional area, however, scales with positive allometry, meaning larger corn snakes have relatively stouter muscles. This result aligns with the findings of at least two previous studies. Penning and Moon (2017) found that the combined cross-sectional area of four epaxial muscles (multifidus, semispinalis-spinalis, longissimus dorsi, and iliocostalis) generally showed positive allometry with body mass in two species of king snakes (*Lampropeltis* spp.) and rat snakes (*Pantherophis* spp.), with some differences depending where along the body the cross-sectional area was measured. Jayne and Riley (2007) found that when regressed on snout-vent length, the cross-sectional areas of the same four epaxial muscles scale with slopes higher than predicted by geometric similarity in the arboreal snake *Boiga irregularis*. Because a muscle's ability to generate force is proportional to its cross-sectional area (McMahon, 1984), that means larger corn snakes likely have disproportionately greater ability to generate force. In support of this hypothesis, one study relating muscle size to force production in a sample of similarly-sized rainbow boas (*Epicrates cenchria*) showed that individual variation in the combined size of the semispinalis-spinalis and longissimus dorsi muscles accounted for half of individual variation in maximum constricting force (Lourdais et al., 2005).

4.4 | Comparison of different methods for computing multiarticular muscle contributions to movement

The reasonably good performance of the simple-distance approach in approximating the results of the cross-product approach bodes well for future research—it could have utility for collecting data non-destructively (e.g., for rare museum specimens, where it isn't possible to destructively sample them to determine muscle lengths) and/or for projects requiring large interspecific datasets where it isn't feasible to dissect all muscles for all species. The simple distance approach naturally performs best for muscles that run parallel to the axis of motion, such as the longissimus dorsi in snakes, but it still produced values within 10% of the cross-product approach for snake epaxial muscles with anterior and posterior attachment points at different

distances from the axis of motion. The simple distance approach performs less well for the hypaxial muscle we examined, the levator costae, which spans only one joint and is steeply angled. However, even for the levator costae, simple distance values were within 18% of the lever arm values.

Monoarticular methods can provide insight into multiarticular systems under the right conditions. However, the core assumptions of monoarticular methods can sometimes produce ambiguous or even contradictory results when applied to multiarticular systems. Our cross-product results provide a stark example of this potential for ambiguity. For monoarticular systems, the position vector ($\vec{r}$) can run from the joint to either muscle attachment and produce a torque vector of the same magnitude. Similarly, one has a choice of attachment points for the position vector ($\vec{r}$) when assessing a multiarticular system. However, multiarticular systems present an additional complication in that the muscle crosses several joints, and as a result, it is unclear which joint should be selected as the origin for $\vec{r}$. We constrained our calculations by setting r_z equal to 0, which is equivalent to a situation where the motion occurs around the intervertebral joint closest to the chosen muscle attachment (i.e., the posterior-most joint when choosing the posterior attachment point for $\vec{r}$). For most muscles, we found that the three options we used for computing $\vec{r}$ (Figure 1c; Methods) led to minor variation in the magnitude of the total lever arms and their relative components, without differences in sign (Figure 3). However, in the case of the iliocostalis pitch component, one choice of $\vec{r}$ predicted that contraction of the iliocostalis would cause dorsal flexion, whereas the other two calculation methods predicted ventral flexion. This discrepancy occurred because the posterior iliocostalis attachment point is slightly dorsal to the vertebral condyle while the anterior iliocostalis attachment is ventral (and at a greater distance). Because we have no fundamental reason to prefer one of the choices of $\vec{r}$ over any other, this discrepancy must be an artifact of applying a monoarticular method to a multiarticular system.

Use of an explicitly multiarticular approach resolves the ambiguity surrounding cross-product results for the iliocostalis, clearly demonstrating that it is a ventral flexor, in contrast to the other three epaxial muscles under consideration (Figure 4). When we consider the system as multiarticular and constrain the vertebral column to bend with constant curvature, contraction of the iliocostalis produces buckling behavior, and the asymmetrical dorsal and ventral lever arms serve to bias the system to ventral bending (Appendix 3 in Supplementary Materials and Methods). Future studies of similar systems should therefore consider whether the two attachment points of the muscle or actuator of interest are located on the same or opposite sides of the axis of motion. When they are located on the same side, then monoarticular methods may reasonably be applied. When they are located on opposite sides, it becomes more important to take an explicitly multiarticular approach. If using the monoarticular cross-product approach, use of the midpoint between the two attachments for calculating the $\vec{r}$ vector can help ensure that the results will capture the correct direction of buckling.

Our curvature approach yields additional insight into multiarticular systems. If a muscle runs along the joints at an angle rather than parallel to the axis of motion, that angle can influence its contributions to curvature, but does not necessarily have a large effect. Because the spirality adjustment of our equation is multiplied by the term $\left(\frac{d_a - d_p}{2L_v \kappa_v}\right)$, the effect of spirality only matters if 1) the muscle attachments are offset from each other by a distance that is reasonably large relative to the length along the axis of motion that the muscle spans, and 2) the curvature is relatively low. Snakes are relatively narrow tubes, so the offset ($d_a - d_p$) is limited, whereas epaxial muscles generally span many joints, so the total length of vertebral column spanned (L_v) is comparatively large. Therefore, the spirality adjustment in our curvature equations makes a negligible difference for the epaxial muscles we examined. We expect that the spirality adjustment can similarly be ignored for some other biological systems where relatively long muscles are confined to relatively narrow tubes, as might be found in tails, for example. However, some multiarticular muscles span modest numbers of joints and/or may slope more steeply because they are not confined to such narrow tubes. For such muscles, the spirality adjustment could be very consequential. Engineered systems lack many of the constraints of biological systems and can take therefore a wide variety of configurations; as a result, the spirality adjustment could make a major difference to function in some engineered systems.

4.5 | Roles of different snake muscles during movement in different planes

Snakes accomplish a remarkable diversity of behaviors using their axial musculature. Different behaviors can involve bending in various planes, and as a result, certain muscles may have greater or less importance depending on the primary plane of motion.

Many behaviors, especially locomotor behaviors, involve lateral flexion. Based on our results, the iliocostalis should be the most important epaxial muscle for lateral flexion, followed by the longissimus dorsi, at least in corn snakes (Table 3; Figure 3). They are likely also the two most important muscles for lateral flexion in other snake species. A study using electromyography (EMG) showed that both of these muscles are active during several types of snake locomotion, including lateral undulation on land, undulatory swimming, sidewinding, and concertina (Jayne,1988a, 1988b). The EMG data also showed activity of the semispinalis-spinalis during these locomotor modes although we demonstrate that its lever arm has a smaller yaw component than do the longissimus dorsi and the iliocostalis, which makes sense given that it is more medially located. The iliocostalis has also been shown to be active during sand swimming in a lizard species, *Scincus scincus* (Sharpe et al., 2013).

Snakes also engage in numerous behaviors that require dorsal flexion. Such behaviors include sidewinding locomotion, which requires a snake to lift sections of its body up and forward (Jayne, 1988a; Mosauer, 1930; Tingle, 2020); vertical undulation

during locomotion (Jurestovsky et al., 2021); defensive displays of cobras and some other taxa, which involve elevating the anterior part of the body (Greene, 1988; Young & Kardong, 2010); male combat behavior in numerous snake families, most famously rattlesnakes (Carpenter, 1986; Missassi et al., 2022; Shaw, 1948); and the lunging or jumping behavior performed by some arboreal snakes as they cross wide gaps between perches or initiate a glide (Byrnes & Jayne, 2012; Socha, 2011). Dorsiflexors also engage to prevent ventral flexion (buckling) as a snake cantilevers itself across a gap between perches (Jayne & Riley, 2007; Jorgensen & Jayne, 2017). Since they are located above the vertebral condyle, and their contraction therefore leads to dorsal flexion, the semispinalis-spinalis, the multifidus, and the longissimus dorsi can all contribute to these behaviors (Table 3; Figure 3). In corn snakes, the semispinalis-spinalis and the multifidus produce about twice as much torque as the longissimus dorsi based on lever arm pitch components and the results of the multiarticular analysis (Table 3; Figures 3 and 4). Therefore, they might play a greater role in dorsal flexion requiring high torque (e.g., bridging gaps while static or quasi-static), whereas the longissimus could be especially important for fast dorsal flexion (e.g., rearing up for a defensive display). Although we know very little about the evolution of epaxial muscles in relation to these behaviors, a phylogenetic comparative analysis of semispinalis-spinalis length demonstrated significantly shorter semispinalis-spinalis muscles in vipers specialized for sidewinding (Tingle et al., 2017), possibly an adaptation enhancing their ability to curve the body more tightly in either the dorsal or lateral plane for a given absolute length change in the semispinalis-spinalis. Future comparative and functional studies could further examine the dorsiflexor morphology and its role in numerous interesting behaviors.

Constriction, used by many snake species to subdue prey, can require lateral flexion or ventral flexion. Snakes can use different postures during constriction, coiling in such a way that either the lateral or ventral surface of the body wraps around the prey (Greene & Burghardt, 1978; Moon, 2000). EMG-recordings for the semispinalis-spinalis, longissimus dorsi, and iliocostalis demonstrate that all three are active during constriction using lateral bends in the gopher snake *Pituophis melanoleucus* (Moon, 2000). Constricting snakes exert high pressure (Boback et al., 2012, 2015; Moon & Mehta, 2007), so one might expect them to evolve longer lever arms. Previous studies have examined the evolution of length with respect to constriction for one muscle, the semispinalis-spinalis (Jayne, 1982; Tingle et al., 2017). They found limited, inconclusive evidence for shorter muscles in constricting species. However, given that our study indicates the iliocostalis may be the most important muscle for both lateral flexion and ventral flexion, future studies of constriction may consider to focus more strongly on it rather than the semispinalis-spinalis. It would also be constructive for future studies relating the evolution of muscle anatomy to constriction to consider differences in constriction posture.

Although the semispinalis-spinalis, multifidus, and iliocostalis are all hypothetically capable of producing torsion of the vertebral column (roll) (Figure 3), previous studies have indicated that the vertebral column is fairly restricted in its twisting ability due to bony processes, which limit roll to approximately 2.5° or less per pair of vertebrae for several species that have been studied (Jurestovsky et al., 2020; Moon, 1999). In contrast, these species have maximal lateral flexion values ranging from 14 to 18.5°, maximal ventral flexion 8.7°–13.5°, and maximal dorsal flexion 4.8°–10.7° (Jurestovsky et al., 2020). The potential role of torsion, if any, for snake behaviors has yet to be shown in vivo, and may be irrelevant due to the limited torsional range of motion.

Muscles can play important roles not only for movement in various planes, but also for stabilization. For example, the human gluteus maximus helps stabilize the hips and trunk during certain activities, and is thought to have evolved its enlarged size primarily due to the importance of its stabilization role (Lieberman et al., 2006; Marzke et al., 1988). Multiarticular muscles may similarly activate in patterns that contribute to stabilization rather than to torque generation. Their function in a given behavior can depend on whether they activate unilaterally or bilaterally. For lateral flexion to occur, as in lateral undulation or concertina locomotion, muscles must activate unilaterally (Jayne,1988a, 1988b). When muscles activate bilaterally, their lateral components cancel out (assuming equal activation), in which case they can act in dorsoventral flexion or as stabilizers (Jayne, 1988a; Jorgensen & Jayne, 2017).

Given the variety of important behaviors that snake epaxial muscles power, muscle anatomy must evolve to allow adequate function of crucial behaviors in the face of functional trade-offs. The torque-speed trade-off for lever arm length exists in both monoarticular and multiarticular muscles: longer lever arms lead to greater torque, but slower movement. Based on Equation (6), one might conclude that decreasing the number of joints a muscle spans would compensate for a longer lever arm, preserving the relationship between absolute muscle shortening and intervertebral joint angle changes. However, muscle speed and range of motion are determined by relative fiber length, which corresponds to muscle span, so muscles spanning fewer joints would have reduced absolute speed and absolute range of motion. Therefore, the complexity of multiarticular muscles does not provide a means for circumventing the torque-speed trade-off. The existence of multiple axial muscles provides an opportunity for some to specialize for high-torque behaviors while others specialize for high-speed behaviors, allowing selective recruitment to adequately meet a range of performance demands. If future studies determine the levels of activation of different muscles during various activities, it would become possible to firmly link the function of different muscles to their morphological evolution across species.

We mainly considered relatively simple muscles, that is, ones running with fibers in a parallel line, and muscle bellies aligned with their tendons. However, the snake semispinalis-spinalis and muscles or actuators in other systems present interesting complications. The semispinalis-spinalis has two muscle bellies, with the semispinalis in line with the anterior tendon and the spinalis off-axis from the tendon (Figure 1a). It's possible for both to be active simultaneously or only one to be active. Activity of the semispinalis alone would tend to move the muscle-tendon unit at an angle, since the anterior attachment is dorsal to the posterior attachment.

Activity of the spinalis, however, would tend to deflect the muscle-tendon unit ventrally. It could therefore cause the muscle-tendon unit to move approximately longitudinally (more-or-less parallel with the vertebral column) instead of at an angle. Additionally, some muscles contain connective tissue that can serve as a septum between different sections of muscle tissue, electrically isolating them and creating the possibility of independent activation (Bodine et al., 1982). Independent activation could have major impacts on function, so for such muscles, it is therefore worth using methods like electromyography or fluoromicrometry to investigate whether they actually function independently.

5 | CONCLUSION

This study makes several contributions to scientific understanding of the anatomy and function of multiarticular trunk muscles. First, we examined whether location along the body affects cross-sectional area or lever arm for any epaxial muscles, an important first step in determining whether regional differences in anatomy might track behaviors that involve only some regions of the body. Second, since size often has major functional consequences for animals and machines, we examined scaling of cross-sectional areas and lever arms. Third, our data allow comparison of the potential contributions of different epaxial muscles to torque in different planes of motion (pitch, yaw, and roll), which provides a baseline for hypotheses regarding the expected evolution of different muscles with respect to snake behavior. Fourth, we provide an analytical tool (our equation relating muscle length change to curvature) that can be used to better understand other multiarticular muscle systems, although it would naturally apply most easily to systems most similar to our own (e.g., vertebral columns lacking dramatic regionalization, other systems involving serially repeated units). For multiarticular systems with specialized features that distinguish them from ours (e.g., vertebral columns of certain clades with dramatic regional specializations, digits or other structures in which each segment has different lengths and lever arms), the fundamental concepts may be useful but any equations would need to be modified to account for those systems' particular features. Finally, between this study and another on muscle sarcomere length in the same species (Jurestovsky et al., 2022), it will now be possible to determine the maximum force that corn snakes can generate, enabling future work on trade-offs between mechanical output and locomotor control.

ACKNOWLEDGMENTS

We thank Andrew Knoll for assistance with μCT scanning. This work was funded by NSF Award #2045581 to HCA.

CONFLICTS OF INTEREST STATEMENT

The authors declare no conflicts of interest.

DATA AVAILABILITY STATEMENT

Image stacks from μCT scans are available on MorphoSource (see Supporting Information File 1 for a spreadsheet containing DOIs). Additional data (specimen measurements, Fiji output) and scripts are provided as supplementary materials.

ORCID

Jessica L. Tingle http://orcid.org/0000-0003-4336-6291

PEER REVIEW

The peer review history for this article is available at https://www.webofscience.com/api/gateway/wos/peer-review/10.1002/jmor.21591.

REFERENCES

Adamczyk, M. M., & Crago, P. E. (2000). Simulated feedforward neural network coordination of hand grasp and wrist angle in a neuroprosthesis. *IEEE Transactions on Rehabilitation Engineering*, *8*, 297–304.

Aerts, P. (1998). Vertical jumping in *Galago senegalensis*: The quest for an obligate mechanical power amplifier. *Philosophical Transactions of the Royal Society of London. Series B: Biological Sciences*, *353*, 1607–1620.

Astley, H. C. (2020). The biomechanics of multi-articular muscle–tendon systems in snakes. *Integrative and Comparative Biology*, *60*, 140–155.

Astley, H. C., & Jayne, B. C. (2009). Arboreal habitat structure affects the performance and modes of locomotion of corn snakes (*Elaphe guttata*). *Journal of Experimental Zoology Part A: Ecological Genetics and Physiology*, *311A*, 207–216.

Backus, S. B., Sustaita, D., Odhner, L. U., & Dollar, A. M. (2015). Mechanical analysis of avian feet: Multiarticular muscles in grasping and perching. *Royal Society Open Science*, *2*, 140350.

Bergmann, P. J., Mann, S. D. W., Morinaga, G., Freitas, E. S., & Siler, C. D. (2020). Convergent evolution of elongate forms in craniates and of locomotion in elongate squamate reptiles. *Integrative and Comparative Biology*, *60*, 190–201.

Boback, S. M., Hall, A. E., McCann, K. J., Hayes, A. W., Forrester, J. S., & Zwemer, C. F. (2012). Snake modulates constriction in response to prey's heartbeat. *Biology Letters*, *8*, 473–476.

Boback, S. M., McCann, K. J., Wood, K. A., McNeal, P. M., Blankenship, E. L., & Zwemer, C. F. (2015). Snake constriction rapidly induces circulatory arrest in rats. *Journal of Experimental Biology*, *218*, 2279–2288.

Bobbert, M. F., & van Ingen Schenau, G. J. (1988). Coordination in vertical jumping. *Journal of Biomechanics*, *21*, 249–262.

Bodine, S. C., Roy, R. R., Meadows, D. A., Zernicke, R. F., Sacks, R. D., Fournier, M., & Edgerton, V. R. (1982). Architectural, histochemical, and contractile characteristics of a unique biarticular muscle: The cat semitendinosus. *Journal of Neurophysiology*, *48*, 192–201.

Böhmer, C., Prevoteau, J., Duriez, O., & Abourachid, A. (2020). Gulper, ripper and scrapper: Anatomy of the neck in three species of vultures. *Journal of Anatomy*, *236*, 701–723.

Byrnes, G., & Jayne, B. C. (2012). The effects of three-dimensional gap orientation on bridging performance and behavior of brown tree snakes (*Boiga irregularis*). *Journal of Experimental Biology*, *215*, 2611–2620.

Carpenter, C. C. (1986). An inventory of combat rituals in snakes. *Smithsonian Herpetological Information Service*, *69*; 1–18.

Cholewicki, J., & VanVliet, J. J., IV (2002). Relative contribution of trunk muscles to the stability of the lumbar spine during isometric exertions. *Clinical Biomechanics*, *17*, 99–105.

Conroy, C., Papenfuss, T., Parker, J., & Hahn, N. (2009). Use of tricaine methanesulfonate (MS222) for euthanasia of reptiles. *Journal of the American Association for Laboratory Animal Science: JAALAS*, *48*, 28–32.

Cromwell, R. L., Aadland-Monahan, T. K., Nelson, A. T., Stern-Sylvestre, S. M., & Seder, B. (2001). Sagittal plane analysis of head, neck, and trunk

kinematics and electromyographic activity during locomotion. *Journal of Orthopaedic & Sports Physical Therapy*, *31*, 255–262.

Doyle, C. E., Bird, J. J., Isom, T. A., Kallman, J. C., Bareiss, D. F., Dunlop, D. J., King, R. J., Abbott, J. J., & Minor, M. A. (2013). An avian-inspired passive mechanism for quadrotor perching. *IEEE/ASME Transactions on Mechatronics*, *18*, 506–517.

Dumas, G. A., Poulin, M. J., Roy, B., Gagnon, M., & Jovanovic, M. (1991). Orientation and moment arms of some trunk muscles. *Spine*, *16*, 293–303.

Fox, J., & Weisberg, S. (2019). *An R companion to applied regression* (3rd ed.). Sage.

Gans, C. (1974). *Biomechanics: An Approach to Vertebrate Biology*. University of Michigan Press.

Gasc, J.-P. (1967). Introduction à l'étude de la musculature axiale des squamates serpentiformes. *Mém Muséum Natl Hist Nat Sér Zool*, *48*, 69–125.

Gasc, J.-P. (1974). L'interprétation fonctionnelle de l'appareil musculo-squelettique de l'axe vertébral chez les serpents (Reptilia). *Mém Muséum Natl Hist Nat Sér Zool*, *83*, 1–182.

Gasc, J.-P. (1981). Axial musculature. In C. Gans & T. S. Parsons, (Eds.), *Biol Reptil* (pp. 355–435). Academic Press.

Gignac, P. M., Kley, N. J., Clarke, J. A., Colbert, M. W., Morhardt, A. C., Cerio, D., Cost, I. N., Cox, P. G., Daza, J. D., Early, C. M., Echols, M. S., Henkelman, R. M., Herdina, A. N., Holliday, C. M., Li, Z., Mahlow, K., Merchant, S., Müller, J., Orsbon, C. P., … Witmer, L. M. (2016). Diffusible iodine-based contrast-enhanced computed tomography (diceCT): An emerging tool for rapid, high-resolution, 3-D imaging of metazoan soft tissues. *Journal of Anatomy*, *228*, 889–909.

Gramsbergen, A., Geisler, H. C., Taekema, H., & van Eykern, L. A. (1999). The activation of back muscles during locomotion in the developing rat. *Developmental Brain Research*, *112*, 217–228.

Gray, J., & Lissmann, H. W. (1950). The kinetics of locomotion of the grass-snake. *Journal of Experimental Biology*, *26*, 354–367.

Greene, H. W., & Burghardt, G. M. (1978). Behavior and phylogeny: Constriction in ancient and modern snakes. *Science*, *200*, 74–77.

Greene, H. W. (1988). Antipredator mechanisms in reptiles. P. In C. Gans & R. B. Huey, (Eds.), *Biol Reptil*. Alan R. Liss, Inc.

Jayne, B. C. (1982). Comparative morphology of the semispinalis-spinalis muscle of snakes and correlations with locomotion and constriction. *Journal of Morphology*, *172*, 83–96.

Jayne, B. C. (1988a). Muscular mechanisms of snake locomotion: An electromyographic study of the sidewinding and concertina modes of *Crotalus cerastes*, *Nerodia fasciata* and *Elaphe obsoleta*. *Journal of Experimental Biology*, *140*, 1–33.

Jayne, B. C. (1988b). Muscular mechanisms of snake locomotion: An electromyographic study of lateral undulation of the florida banded water Snake (*Nerodia fasciata*) and the yellow rat Snake (*Elaphe obsoleta*). *Journal of Morphology*, *197*, 159–181.

Jayne, B. C. (2020). What defines different modes of snake locomotion? *Integrative and Comparative Biology*, *60*, 156–170.

Jayne, B. C., & Riley, M. A. (2007). Scaling of the axial morphology and gap-bridging ability of the brown tree Snake, *Boiga irregularis*. *Journal of Experimental Biology*, *210*, 1148–1160.

Jorgensen, R. M., & Jayne, B. C. (2017). Three-dimensional trajectories affect the epaxial muscle activity of arboreal snakes crossing gaps. *Journal of Experimental Biology*, *220*. jeb.164640.

Jurestovsky, D. J., Jayne, B. C., & Astley, H. C. (2020). Experimental modification of morphology reveals the effects of the zygosphene–zygantrum joint on the range of motion of snake vertebrae. *Journal of Experimental Biology*, *223*, jeb216531.

Jurestovsky, D. J., Tingle, J. L., & Astley, H. C. (2022). Corn snakes show consistent sarcomere length ranges across muscle groups and ontogeny. *Integrative Organismal Biology*, *4*, obac040.

Jurestovsky, D. J., Usher, L. R., & Astley, H. C. (2021). Generation of propulsive force via vertical undulations in snakes. *Journal of Experimental Biology*, *224*, jeb239020.

Kano, T., Sato, T., Kobayashi, R., & Ishiguro, A. 2011. Decentralized control of multi-articular snake-like robot for efficient locomotion. 1875–1880 in 2011 IEEERSJ Int Conf Intell Robots Syst. Presented at the 2011 IEEE/RSJ International Conference on Intelligent Robots and Systems (IROS 2011), IEEE, San Francisco, CA.

Kong, Y. S., Cho, Y. H., & Park, J. W. (2013). Changes in the activities of the trunk muscles in different kinds of bridging exercises. *Journal of Physical Therapy Science*, *25*, 1609–1612.

Lee, S. W., Vermillion, B. C., Geed, S., Dromerick, A. W., & Kamper, D. G. (2018). Impact of targeted assistance of multiarticular finger musculotendons on the coordination of finger muscles during isometric force production. *IEEE Transactions on Neural Systems and Rehabilitation Engineering*, *26*, 619–628.

Lemelin, P. (1995). Comparative and functional myology of the prehensile tail in new world monkeys. *Journal of Morphology*, *224*, 351–368.

Lieber, R. L., & Boakes, J. L. (1988). Sarcomere length and joint kinematics during torque production in frog hindlimb. *American Journal of Physiology-Cell Physiology*, *254*, C759–C768.

Lieberman, D. E., Raichlen, D. A., Pontzer, H., Bramble, D. M., & Cutright-Smith, E. (2006). The human gluteus maximus and its role in running. *Journal of Experimental Biology*, *209*, 2143–2155.

Lourdais, O., Brischoux, F., & Barantin, L. (2005). How to assess musculature and performance in a constricting snake? A case study in the Colombian Rainbow Boa (*Epicrates cenchria maurus*). *Journal of Zoology*, *265*, 43–51.

Luger, A. M., Ollevier, A., De Kegel, B., Herrel, A., & Adriaens, D. (2020). Is variation in tail vertebral morphology linked to habitat use in chameleons? *Journal of Morphology*, *281*, 229–239.

Luger, A. M., Watson, P. J., Dutel, H., Fagan, M. J., Van Hoorebeke, L., Herrel, A., & Adriaens, D. (2021). Regional patterning in tail vertebral form and function in chameleons (*Chamaeleo calyptratus*). *Integrative and Comparative Biology*, *61*, 455–463.

Macintosh, J. E., Bogduk, N., & Pearcy, M. J. (1993). The effects of flexion on the geometry and actions of the lumbar erector spinae. *Spine*, *18*, 884–893.

Manzano, A. S., Abdala, V., & Herrel, A. (2008). Morphology and function of the forelimb in arboreal frogs: Specializations for grasping ability? *Journal of Anatomy*, *213*, 296–307.

Marzke, M. W., Longhill, J. M., & Rasmussen, S. A. (1988). Gluteus maximus muscle function and the origin of hominid bipedality. *American Journal of Physical Anthropology*, *77*, 519–528.

McMahon, T. A. (1984). *Muscles, reflexes, and locomotion*. Princeton University Press.

Missassi, A. F. R., Coeti, R. Z., Almeida-Santos, S. M., & Prudente, A. L. C. (2022). Intense male-male ritual combat in the *Micrurus ibiboboca* complex (Elapidae) from northeastern South America. *Herpetological Conservation and Biology*, *17*, 204–216.

Moon, B. R. (1999). Testing an inference of function from structure: Snake vertebrae do the twist. *Journal of Morphology*, *241*, 217–225.

Moon, B. R. (2000). The mechanics and muscular control of constriction in Gopher snakes (*Pituophis melanoleucus*) and a king Snake (*Lampropeltis getula*). *Journal of Zoology*, *252*, 83–98.

Moon, B. R., & Mehta, R. S. (2007). Constriction strength in snakes. In R. W. Henderson & R. Powell, (Eds.), *Biol boas pythons* (pp. 207–212). Eagle Mountain Publishing LC.

Mosauer, W. (1930). A note on the sidewinding locomotion of snakes. *The American Naturalist*, *64*, 179–183.

Mosauer, W. (1935). The myology of the trunk region of snakes and its significance for ophidian taxonomy and phylogeny. *Publ Univ Calif Los Angel Biol Sci*, *1*, 81–120.

Newman, S. J., & Jayne, B. C. (2018). Crawling without wiggling: Muscular mechanisms and kinematics of rectilinear locomotion in Boa constrictors. *Journal of Experimental Biology*, *221*, 1–12.

Nicodemo, P. (2012). Longitudinal variation in the axial muscles of snakes *(Master's)*. University of Cincinnati.

Nuzzo, J. L., McCaulley, G. O., Cormie, P., Cavill, M. J., & McBride, J. M. (2008). Trunk muscle activity during stability ball and free weight exercises. *Journal of Strength and Conditioning Research*, *22*, 95–102.

O'Reilly, J. C., Summers, A. P., & Ritter, D. A. (2000). The evolution of the functional role of trunk muscles during locomotion in adult amphibians. *American Zoologist*, *40*, 123–135.

Omura, A., Ejima, K. I., Honda, K., Anzai, W., Taguchi, Y., Koyabu, D., & Endo, H. (2015). Locomotion pattern and trunk musculoskeletal architecture among Urodela. *Acta Zoologica*, *96*, 225–235.

Organ, J. M. (2007). *The functional anatomy of prehensile and nonprehensile tails of the Platyrrhini (Primates) and Procyonidae (Carnivora)* (Doctoral). Johns Hopkins University, Baltimore, Maryland.

Penning, D. A. (2018). Quantitative axial myology in two constricting snakes: *Lampropeltis holbrooki* and *Pantherophis obsoletus*. *Journal of Anatomy*, *232*, 1016–1024.

Penning, D. A., & Moon, B. R. (2017). The king of snakes: Performance and morphology of intraguild predators (*Lampropeltis*) and their prey (*Pantherophis*). *Journal of Experimental Biology*, *220*, 1154–1161.

Pollard, N. S., & Gilbert, R. C. (2002). Tendon arrangement and muscle force requirements for human-like force capabilities in a robotic finger. 3755–3762 Proc 2002 IEEE Int Conf Robot Autom Cat No02CH37292. Presented at the 2002 IEEE International Conference on Robotics and Automation, IEEE, Washington, DC, USA.

Pregill, G. K. (1977). Axial myology of the racer *Coluber-constrictor* with emphasis on the neck region. *Transactions of the San Diego Society of Natural History*, *18*, 185–206.

R Core Team. (2022). *R: A language and environment for statistical computing*. R Foundation for Statistical Computing.

Ramos, A. M., & Walker, I. D. (1998). Raptors-inroads to multifingered grasping. 467–475 in Proc 1998 IEEERSJ Int Conf Intell Robots Syst Innov Theory Pract Appl Cat No98CH36190. Presented at the Proceedings. 1998 IEEE/RSJ International Conference on Intelligent Robots and Systems. Innovations in Theory, Practice and Applications, IEEE, Victoria, BC, Canada.

Ritter, D. (1992). Lateral bending during lizard locomotion. *Journal of Experimental Biology*, *173*, 1–10.

Ruben, J. A. (1977). Morphological correlates of predatory modes in the coachwhip (*Masticophis flagellum*) and Rosy Boa (*Lichanura roseofusca*). *Herpetologica*, *33*, 1–6.

Saab, W., Rone, W. S., & Ben-Tzvi, P. (2018). Robotic tails: A state-of-the-art review. *Robotica*, *36*, 1263–1277.

Saunders, S. W., Rath, D., & Hodges, P. W. (2004). Postural and respiratory activation of the trunk muscles changes with mode and speed of locomotion. *Gait & Posture*, *20*, 280–290.

Schiebel, P. E., Hubbard, A. M., & Goldman, D. I. (2020). Comparative study of snake lateral undulation kinematics in model heterogeneous terrain. *Integrative and Comparative Biology*, icaa125.

Schilling, N., & Carrier, D. R. (2010). Function of the epaxial muscles in walking, trotting and galloping dogs: Implications for the evolution of epaxial muscle function in tetrapods. *Journal of Experimental Biology*, *213*, 1490–1502.

Schindelin, J., Arganda-Carreras, I., Frise, E., Kaynig, V., Longair, M., Pietzsch, T., Preibisch, S., Rueden, C., Saalfeld, S., Schmid, B., Tinevez, J. Y., White, D. J., Hartenstein, V., Eliceiri, K., Tomancak, P., & Cardona, A. (2012). Fiji: An open-source platform for biological-image analysis. *Nature Methods*, *9*, 676–682.

Sharpe, S. S., Ding, Y., & Goldman, D. I. (2013). Environmental interaction influences muscle activation strategy during sand-swimming in the sandfish lizard *Scincus scincus*. *Journal of Experimental Biology*, *216*, 260–274.

Shaw, C. E. (1948). The male combat "dance" of some crotalid snakes. *Herpetologica*, *4*, 137–145.

Sherratt, E., Coutts, F. J., Rasmussen, A. R., & Sanders, K. L. (2019). Vertebral evolution and ontogenetic allometry: The developmental basis of extreme body shape divergence in microcephalic sea snakes. *Evolution & Development*, *21*, 135–144.

Sherratt, E., & Sanders, K. L. (2020). Patterns of intracolumnar size variation inform the heterochronic mechanisms underlying extreme body shape divergence in microcephalic sea snakes. *Evolution & Development*, *22*, 283–290.

Socha, J. J. (2011). Gliding flight in *Chrysopelea*: Turning a snake into a wing. *Integrative and Comparative Biology*, *51*, 969–982.

Sustaita, D., Pouydebat, E., Manzano, A., Abdala, V., Hertel, F., & Herrel, A. (2013). Getting a grip on tetrapod grasping: Form, function, and evolution: Grasping in tetrapods. *Biological Reviews*, *88*, 380–405.

Tingle, J. L. (2020). Facultatively sidewinding snakes and the origins of locomotor specialization. *Integrative and Comparative Biology*, *60*, 202–214.

Tingle, J. L., Gartner, G. E. A., Jayne, B. C., & Garland, T. (2017). Ecological and phylogenetic variability in the spinalis muscle of snakes. *Journal of Evolutionary Biology*, *30*, 2031–2043.

Valero-Cuevas, F. J. (2005). An integrative approach to the biomechanical function and neuromuscular control of the fingers. *Journal of Biomechanics*, *38*, 673–684.

van der Leeuw, A. H. J., Bout, R. G., & Zweers, G. A. (2001). Control of the cranio-cervical system during feeding in birds. *American Zoologist*, *41*, 1352–1363.

van Ingen Schenau, G. J. (1989). From rotation to translation: Constraints on multi-joint movements and the unique action of bi-articular muscles. *Human Movement Science*, *8*, 301–337.

van Ingen Schenau, G. J., Pratt, C. A., & Macpherson, J. M. (1994). Differential use and control of mono- and biarticular muscles. *Human Movement Science*, *13*, 495–517.

Wiens, J. J., Brandley, M. C., & Reeder, T. W. (2006). Why does a trait evolve multiple times within a clade? Repeated evolution of snakelike body form in squamate reptiles. *Evolution*, *60*, 123–141.

Young, B. A., & Kardong, K. V. (2010). The functional morphology of hooding in cobras. *Journal of Experimental Biology*, *213*, 1521–1528.

SUPPORTING INFORMATION

Additional supporting information can be found online in the Supporting Information section at the end of this article.

How to cite this article: Tingle, J. L., Jurestovsky, D. J., & Astley, H. C. (2023). The relative contributions of multiarticular snake muscles to movement in different planes. *Journal of Morphology*, *284*, e21591. https://doi.org/10.1002/jmor.21591